

See discussions, stats, and author profiles for this publication at: <https://www.researchgate.net/publication/271331573>

Design, Synthesis, and Structure–Activity Relationship of Novel LSD1 Inhibitors Based on Pyrimidine–Thiourea Hybrids As Potent, Orally Active Antitumor Agents

ARTICLE *in* JOURNAL OF MEDICINAL CHEMISTRY · JANUARY 2015

Impact Factor: 5.45 · DOI: 10.1021/acs.jmedchem.5b00037 · Source: PubMed

CITATIONS

2

READS

71

18 AUTHORS, INCLUDING:



[Yi-Chao Zheng](#)

Zhengzhou University

12 PUBLICATIONS 64 CITATIONS

[SEE PROFILE](#)



[Bo Wang](#)

Zhengzhou University

3 PUBLICATIONS 6 CITATIONS

[SEE PROFILE](#)



[Wen Zhao](#)

7 PUBLICATIONS 35 CITATIONS

[SEE PROFILE](#)



[Hong-Min Liu](#)

Zhengzhou University

176 PUBLICATIONS 1,449 CITATIONS

[SEE PROFILE](#)

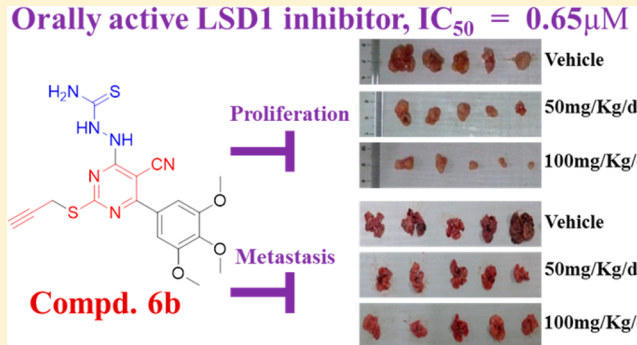
Design, Synthesis, and Structure–Activity Relationship of Novel LSD1 Inhibitors Based on Pyrimidine–Thiourea Hybrids As Potent, Orally Active Antitumor Agents

Li-Ying Ma,[†] Yi-Chao Zheng,[†] Sai-Qi Wang,[†] Bo Wang, Zhi-Ru Wang, Lu-Ping Pang, Miao Zhang, Jun-Wei Wang, Lina Ding, Juan Li, Cong Wang, Biao Hu, Ying Liu, Xiao-Dan Zhang, Jia-Jia Wang, Zhi-Jian Wang, Wen Zhao,* and Hong-Min Liu*

Key Laboratory of Advanced Pharmaceutical Technology, Ministry of Education of China, Co-innovation Center of Henan Province for New Drug R & D and Preclinical Safety, and School of Pharmaceutical Sciences, Zhengzhou University, 100 Kexue Avenue, Zhengzhou, Henan 450001, China

Supporting Information

ABSTRACT: Histone lysine specific demethylase 1 (LSD1) was reported to be overexpressed in several human cancers and recognized as a promising anticancer drug target. In the current study, we designed and synthesized a novel series of pyrimidine–thiourea hybrids and evaluated their potential LSD1 inhibitory effect. One of the compounds, **6b**, containing a terminal alkyne appendage, was shown to be the most potent and selective LSD1 inhibitor *in vitro* and exhibited strong cytotoxicity against LSD1 overexpressed gastric cancer cells. Compound **6b** also showed marked inhibition of cell migration and invasion as well as significant *in vivo* tumor suppressing and antimetastasis role, without significant side effects by oral administration. Our findings indicate that the pyrimidine–thiourea-based LSD1 inactivator may serve as a leading compound targeting LSD1 overexpressed cancers.



■ INTRODUCTION

Histone lysine methylation, a kind of epigenetically covalent modification, can be dynamically regulated through histone methyltransferase and demethylase. Lysine specific demethylase 1 (LSD1), the first identified histone demethylase in 2004,¹ can demethylate mono- and dimethylated K4 and K9 of histone 3 through flavin adenine dinucleotide (FAD)-dependent enzymatic oxidation. It has also been shown to demethylate modified lysine in nonhistone proteins, including p53, E2F transcription factor 1, and DNA methyltransferases (DNMTs) and further regulates their downstream cellular function.² The level of LSD1 expression or its activity has been reported to be upregulated in a variety of human cancers including gastric cancer, prostate cancer, lung cancer, and breast cancer.³ Downregulation or inhibition of LSD1 may have therapeutic potential in cancer. Therefore, it would be of considerable interest to develop LSD1-specific inhibitors for elucidating in detail the biological functions of the enzyme.

To date, several classes of LSD1 inhibitors have been identified, including 2-PCPA derivatives, peptides, polyamine analogues, amidoxime-based compounds, amidino guanidinium compounds, and others.^{4–13} However, highly selective LSD1 inhibitors with strong cytotoxicity against cancer and less side effect remain to be discovered.

As reported, the nitrogen-containing class of compounds such as pyrimidine, triazole, peptide, and tetrazole that are found in many natural products are the important constituents of a number of modern drugs.^{14–30} Among these azole heterocyclics, pyrimidine attracted our attention due to its wide application as monoamine oxidase (MAO) inhibitors,^{31–34} as well as its easy accessibility. Mechanistically and structurally, LSD1 is also related to the flavin-dependent monoamine oxidases. Their similarity in the catalytic and structural properties prompted the investigation of anti-MAO drugs as potential LSD1 inhibitors.³⁵ It was found that several monoamine oxidase inhibitors such as tranylcypromine (2-PCPA) and pargyline are known LSD1 inhibitors, and several reported inhibitors are derivatives of these scaffolds with increased selectivity for LSD1.^{36–41} In addition, polyamine analogues with thiourea moiety,^{42–44} peptides with propargyl moiety, and pargyline^{45–47} showed potent inhibition to LSD1 activity (Figure 1). Furthermore, molecular hybridization, which covalently combines two or more drug pharmacophores into a single molecule, is an emerging structural modification tool to design new molecules with improved pharmacophoric properties. The hybrids may also minimize the unwanted side

Received: September 9, 2014

Published: January 22, 2015



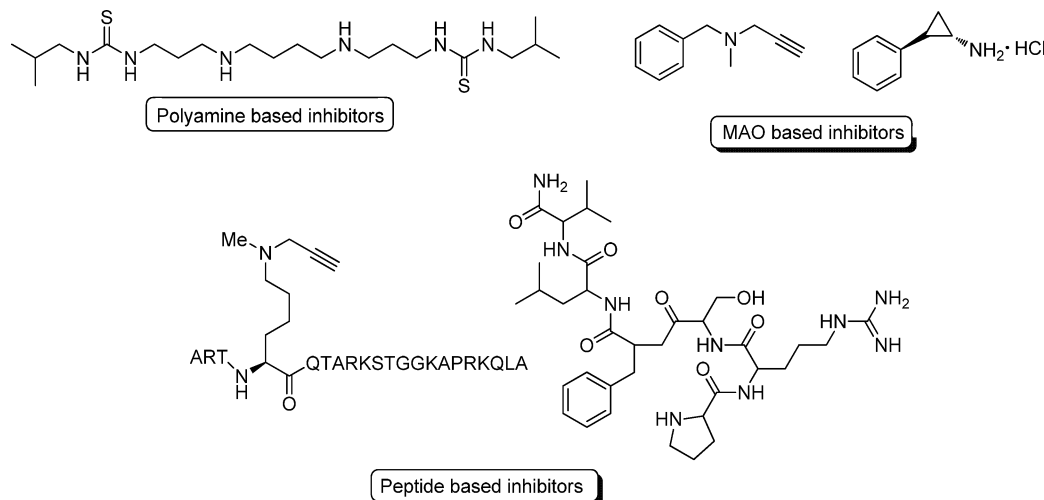
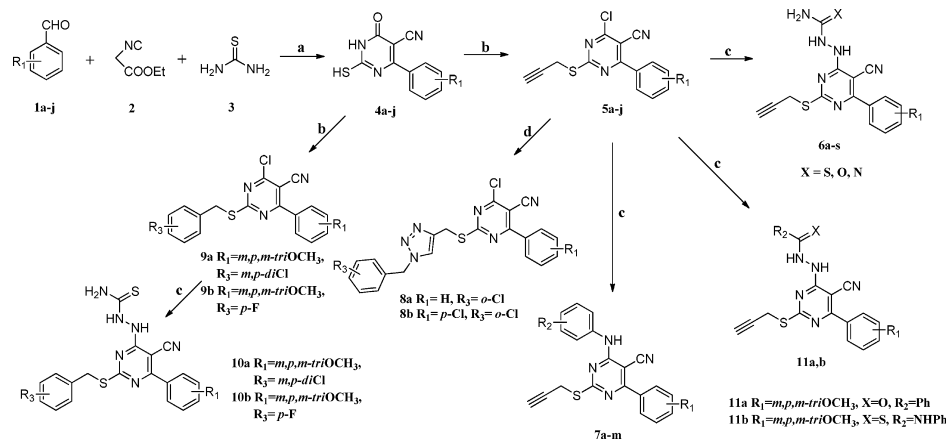


Figure 1. Representative examples of LSD1 inhibitors.

Scheme 1. Synthesis of the Target Pyrimidine–Thiourea Hybrids^a

^aReagents and conditions: (a) absolute ethanol, absolute K_2CO_3 , reflux, 10 h; (b) (i) propargyl bromide, dioxane, reflux; (ii) phosphorus oxychloride, reflux, 1 h; (c) appropriate aniline, absolute ethanol, reflux, 6 h; (d) $\text{CuSO}_4 \cdot 5\text{H}_2\text{O}$, sodium ascorbate, tetrahydrofuran (THF)– H_2O (1:1), room temperature (rt).

effects and allow for synergic action.^{48–54} Therefore, based on the concept of molecular hybridization, we designed a series of small molecules as potential LSD1 inhibitors, taking the key pharmacophoric features aminothiourea and propargyl into account, being linked through a pyrimidine moiety. Compared to 2-PCPA, most of the target compounds, especially compound 6b, exhibited more potent inhibition of LSD1 activity and the cancer cell proliferation with LSD1 over-expression.

■ CHEMISTRY

The general route for the synthesis of the target pyrimidine–thiourea hybrids is depicted in Scheme 1. The 6-aryl-5-cyano-2-thiouracils 4a–j were prepared via prolonged heating of benzaldehydes 1a–j, ethylcyanoacetate 2, and thiourea 3 using potassium carbonate in ethanol.⁵⁵ Compounds 4a–j were allowed to react with the appropriate substituted benzyl chloride, propargyl bromide, and phosphorus oxychloride in dioxane to yield the target derivatives 5a–j and 9a–b. These highly activated intermediates were then reacted with amino-thiourea, aminothiourea, aminoguanidine, and different arylamines to obtain compounds 6a–s, 7a–m, 10a–b, and 11a–b. 8a–b

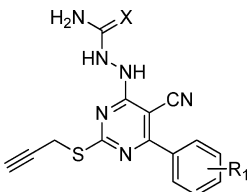
were prepared via click reaction of compound 5a with appropriate substituted benzyl azides. The substituted benzyl azides were readily synthesized from the corresponding halides and sodium azide following literature procedures.^{56,57}

■ RESULTS AND DISCUSSION

Biochemical Activity of the Candidate Compounds against LSD1 and the Structure–Activity Relationship (SAR) Studies. All the compounds synthesized in this study were examined for their inhibitory effect on LSD1 activity in vitro, as reported by our laboratory.⁵⁸ 2-PCPA was chosen as a positive control. The results are summarized in Tables 1–4.

The results of compounds 6a–k against LSD1 were determined initially and shown in Table 1. All the compounds exhibit moderate to good potency with IC_{50} values ranging from 0.65 to 3.58 μM . Among them, compound 6b shows the most potent activity to LSD1 (0.65 μM), which is 42 times stronger than that of 2-PCPA (27.83 μM). During the SAR studies, we found that the hetero atoms substitution on the urea moiety was important for the inhibitory activity: the thiourea derivative compound 6f (2.58 μM) was more potent than the urea derivative compound 6q (11.19 μM), and the

Table 1. Structures of Compounds 6a–s and Their Inhibition Rates (IC_{50}) to the Purified LSD1 Recombinant In Vitro



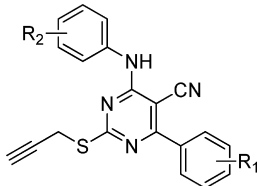
compd	R ₁	X	LSD1 (μ M)
6a	H	S	1.59 ± 0.22
6b	<i>m,p,m</i> -tri-OCH ₃	S	0.65 ± 0.12
6c	<i>p</i> -CH ₃	S	1.10 ± 0.29
6d	<i>p</i> -CH ₂ (CH ₃) ₂	S	1.08 ± 0.03
6e	<i>p</i> -F	S	1.82 ± 0.26
6f	<i>p</i> -NO ₂	S	2.58 ± 0.23
6g	<i>p</i> -Cl	S	1.59 ± 0.20
6h	<i>m,p</i> -di-F	S	1.66 ± 0.22
6i	<i>p</i> -Br	S	1.59 ± 0.20
6j	<i>m</i> -Cl	S	3.58 ± 0.57
6k	<i>m</i> -OCH ₃	S	2.61 ± 0.41
6l	<i>p</i> -Cl	O	2.64 ± 0.42
6m	<i>m,p</i> -di-F	O	7.40 ± 0.87
6n	<i>p</i> -CH ₃	O	3.16 ± 0.51
6o	<i>p</i> -CH ₂ (CH ₃) ₂	O	4.88 ± 0.68
6p	<i>m</i> -Cl	O	5.06 ± 0.70
6q	<i>p</i> -NO ₂	O	11.19 ± 1.04
6r	<i>p</i> -Br	O	41.51 ± 1.61
6s	<i>p</i> -NO ₂	N	>125
2-PCPA			27.83 ± 2.64

guanidine derivative compound 6s without any detectable activity.

To evaluate the importance of aminothiourea moiety for LSD1 inhibitory activity, compounds 7a–m and 5a–j were synthesized and the results are shown in Tables 2 and 3, respectively. Replacing the aminothiourea scaffold with substituted anilines 7a–m (Table 2) led to a complete loss of activity, which suggested that the steric hindrance around the pyrimidine ring may play an important role in determining its inhibitory activity to LSD1. Substitution of aminothiourea scaffold with chlorine atom resulted in an inordinate loss of activity for compounds 5a–j. Those results indicated the significance of the aminothiourea group in retaining their activity. In addition, the role of pyrimidine scaffold in compounds 5a–j was also investigated (Table 3). Some of them show moderate to good activity with IC_{50} ranging from 3.13 to 59.16 μ M. Among them, compounds 5b and 5g were more potent than the corresponding compounds 7l and 7i but less potent than 6b and 6g. These findings indicate that the pyrimidine scaffold may contribute to their inhibitory activity. However, to further prove the SAR of pyrimidine scaffold, it should be better to design and synthesize more targeted compounds with or without the scaffold, which will be investigated in our coming work.

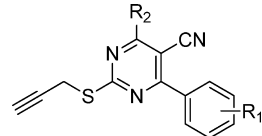
The importance of the propargyl group of our compounds on LSD1 inhibitory activity was also explored (Table 4). The Szewczuk group reported that N₅ of the flavin proforms nucleophilic attack to the propargyl scaffold of an inactivator of LSD1.⁴⁶ To further prove the importance of the propargyl group of our compounds on LSD1 inhibitory activity, we

Table 2. Structure of Compounds 7a–m and Their Inhibition Rates (IC_{50}) to the Purified LSD1 Recombinant In Vitro



compd	R ₁	R ₂	LSD1 (μ M)
7a	H	<i>m</i> -CF ₃	>125
7b	H	<i>p</i> -Cl	>125
7c	H	<i>m</i> -Cl	>125
7d	H	<i>p</i> -F	>125
7e	H	<i>p</i> -NO ₂	>125
7f	H	<i>o</i> -Cl	>125
7g	H	<i>p</i> -CH ₃	>125
7h	H	<i>p</i> -OCH ₃	>125
7i	<i>p</i> -Cl	<i>p</i> -OCH ₃	>125
7j	<i>p</i> -Cl	<i>m</i> -CF ₃	>125
7k	<i>p</i> -Br	<i>p</i> -Cl	>125
7l	<i>m,p,m</i> -tri-OCH ₃	<i>p</i> -OCH ₃	>125
7m	<i>m,p,m</i> -tri-OCH ₃	<i>m</i> -CF ₃	>125

Table 3. Structure of Compounds 5a–j and Their Inhibition Rates (IC_{50}) to the Purified LSD1 Recombinant In Vitro



compd	R ₁	R ₂	LSD1 (μ M)
5a	H	Cl	45.75 ± 0.58
5b	<i>m,p,m</i> -tri-OCH ₃	Cl	3.13 ± 0.49
5c	<i>p</i> -CH ₃	Cl	59.16 ± 1.77
5d	<i>p</i> -CH ₂ (CH ₃) ₂	Cl	26.48 ± 1.42
5e	<i>p</i> -F	Cl	21.82 ± 1.33
5f	<i>p</i> -NO ₂	Cl	>125
5g	<i>p</i> -Cl	Cl	8.33 ± 0.63
5h	<i>m,p</i> -di-F	Cl	24.37 ± 1.38
5i	<i>p</i> -Br	Cl	24.71 ± 1.39
5j	<i>m</i> -Cl	Cl	>125

replaced the propargyl group with phenyl and triazole (non or poor Michael addition receptor), respectively. Their LSD1 inhibitory effects were also evaluated. As can be seen from Table 4, due to the change of the propargyl group to benzyl group, compounds 10a–b exhibit weak or no LSD1 inhibitory effect, compared to the corresponding compound 6b. Replacing the propargyl group by triazole (as in 8a–b) via click chemistry causes a dramatic loss of activity, compared to the corresponding compounds 5a and 5g. These modifications and SAR studies reveal that the propargyl group is critical for their inhibitory activity.

In Vitro Inhibition Properties of Compound 6b to the Recombinant LSD1 and Its Homologues: MAO-A and MAO-B. Because compound 6b exhibits potent LSD1 inhibitory activity in vitro, we further characterized the selectivity of this compound against two LSD1 homologues, MAO-A and MAO-B, as described before.⁵⁸ We found that compound 6b did not show any significant inhibitory effect on

Table 4. Structure of Compounds 8a–b and 10a–b and Their Inhibition Rates (IC_{50}) to the Purified LSD1 Recombinant In Vitro

Compd	R ₁	R ₂	R ₃	LSD1(μM)
5a	H	Cl		45.75±0.58
8a	H	Cl		>125
5g	p-Cl	Cl		8.33±0.63
8b	p-Cl	Cl		>125
6b	<i>m,p,m-triOCH₃</i>			0.65±0.12
10a	<i>m,p,m-triOCH₃</i>			98.57±1.99
10b	<i>m,p,m-triOCH₃</i>			>125

MAO-A and MAO-B, compared to the positive control, 2-PCPA (Figure 2A). Our findings indicate that compound **6b** is a highly selective LSD1 inhibitor.

Furthermore, the inhibitory properties of compound **6b** to LSD1 were determined. Time-dependent assay suggested that, within 8 min, the compound at different concentrations (0.5, 2.0, and 8.0 μM) performed time-dependent inhibitory effect against LSD1. After 8 min, the inhibitory effect remained stable and constant (Figure 2B). To further prove the binding property of compound **6b** to LSD1 recombinant, the mixture of

the compound and LSD1 recombinant was subjected to ultrafiltration and loaded to a Triple-TOF 4600 system. Nevertheless, the peak of the combined compound **6b**–LSD1 was not found (data not shown). A further experiment was also carried out with biolayer interferometry (BLI) to confirm whether there is a direct interaction between the small-molecule and the LSD1 recombinant or not. Figure 2C features the BLI dose–response curve of compounds **6b** to LSD1. Compound **6b** performed a direct interaction with LSD1 at $K_d = 3.7 \mu\text{M}$, which is 27 times higher than the positive control 2-PCPA ($K_d = 101.0 \mu\text{M}$). As can be seen from Figure 2C, after fully binding to LSD1 with increased response, compound **6b** can be dissociated from the recombinant gradually with decreased response. Taken together, these findings demonstrate that compound **6b** may tightly but reversibly bind to LSD1.

Effects of Compounds **6b and **6d** on LSD1 Activity in Gastric Cancer Cells.** To determine the inhibitory effect of compounds **6b** and **6d** on LSD1 activity at the cellular level, a gastric cancer cell line, MGC-803, was chosen. We found that the methylation levels of LSD1 substrates, H3K4me1/me2 and H3K9me2, were dose dependently elevated after compound **6b** and **6d** treatment, whereas H3K4me3, substrate of histone demethylase JARID1, LSD1, and H4 were kept unchanged (Figure 2D and E). These results imply that compounds **6b** and **6d** specifically inhibit LSD1 activity at the cellular level.

Effects of Compound **6b on Gastric Cancer Cell Growth.** We have previously reported that LSD1 was overexpressed in some low differentiated gastric cancer cell lines, including MGC-803 and HGC-27.⁵⁸ To further determine whether compound **6b** is a potential candidate for a chemotherapeutic agent against those gastric cancer cells, in

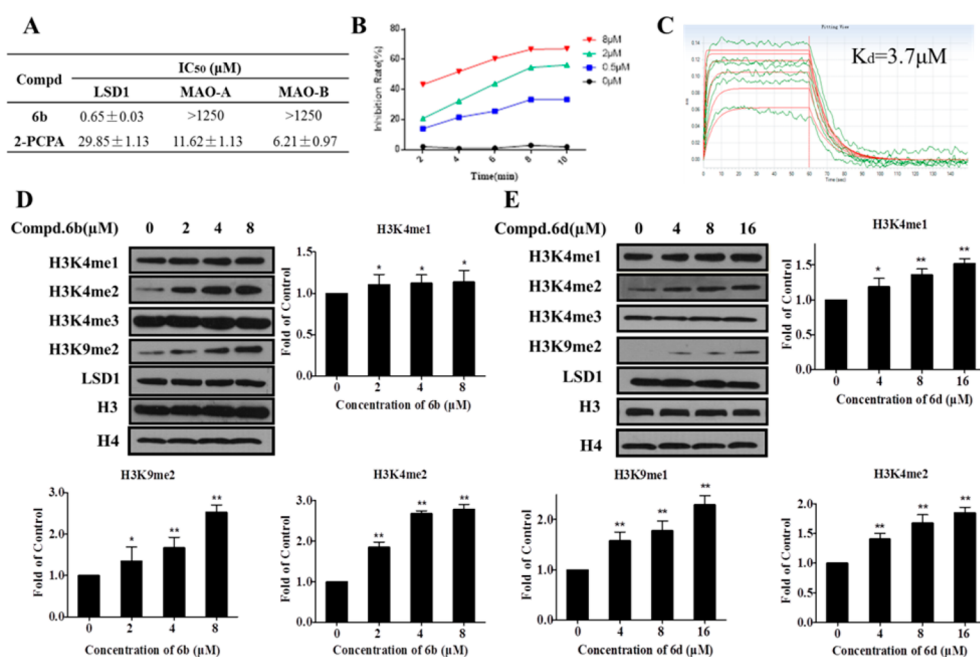


Figure 2. Properties of compounds **6b** and **6d**'s inhibitory effect to LSD1 activity in vitro. (A) Inhibitory effects of compounds **6b** to LSD1 and its homologues, MAO-A and MAO-B. (B) Time-dependent assay of compound **6b** against LSD1. The progress curves for the inactivation of LSD1 were obtained by indicated concentrations of compound **6b** treatment. (C) BLI dose–response curves of compound **6b** (concentrations 100, 50, 25, 12.5, 6.25, and 3.125 μM). (D and E) Histone methylation in MGC-803 cells after treatment by compound **6b** (D) and **6d** (E) for 48 h. The expressions of H3K4me1, me2, H3K9me2, and H4 were determined by Western blot. The total levels of histone 3 (H3) were used as loading control. Data are the mean ± SD. (*) $P < 0.05$ was considered significant. (**) $P < 0.01$ was considered statistically highly significant. All experiments were carried out at least three times.

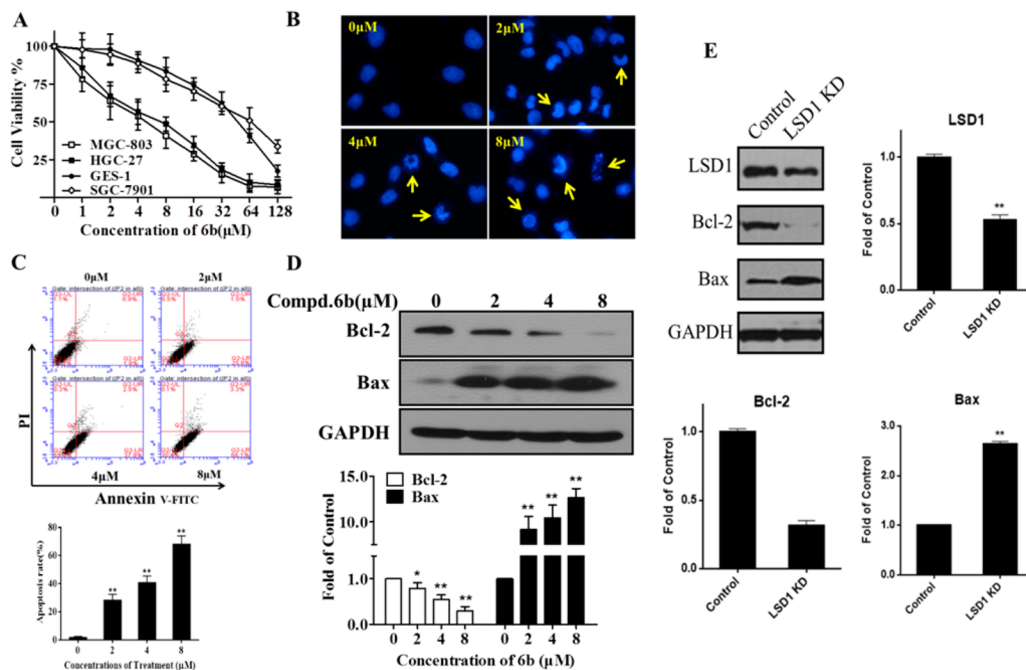


Figure 3. Compound 6b selectively inhibited cell proliferation and induced cell apoptosis. (A) Cytotoxicities of compound 6b on three gastric cancer cell lines, MGC-803, HGC-27, and SGC-7901, and normal gastric epithelial cell line GES-1 were determined by 3-(4,5-dimethylthiazol-2-yl)-2,5-diphenyltetrazolium bromide (MTT) assay. (B) Hoechst-33258 staining was used for apoptotic nuclear morphological analysis after 24 h treatment of compound 6b in MGC-803. (C) Flow cytometry was used for quantitative analysis of cell apoptosis, using an AnnexinV-FITC/PI double staining kit. (D) Expressions of Bcl-2 and Bax were determined after 48 h treatment of compound 6b. (E) Expressions of LSD1, Bcl-2, and Bax were determined after LSD1 was knocked down with siRNA for 48 h. (*) $P < 0.05$ was considered significant. (**) $P < 0.01$ was considered statistically highly significant.

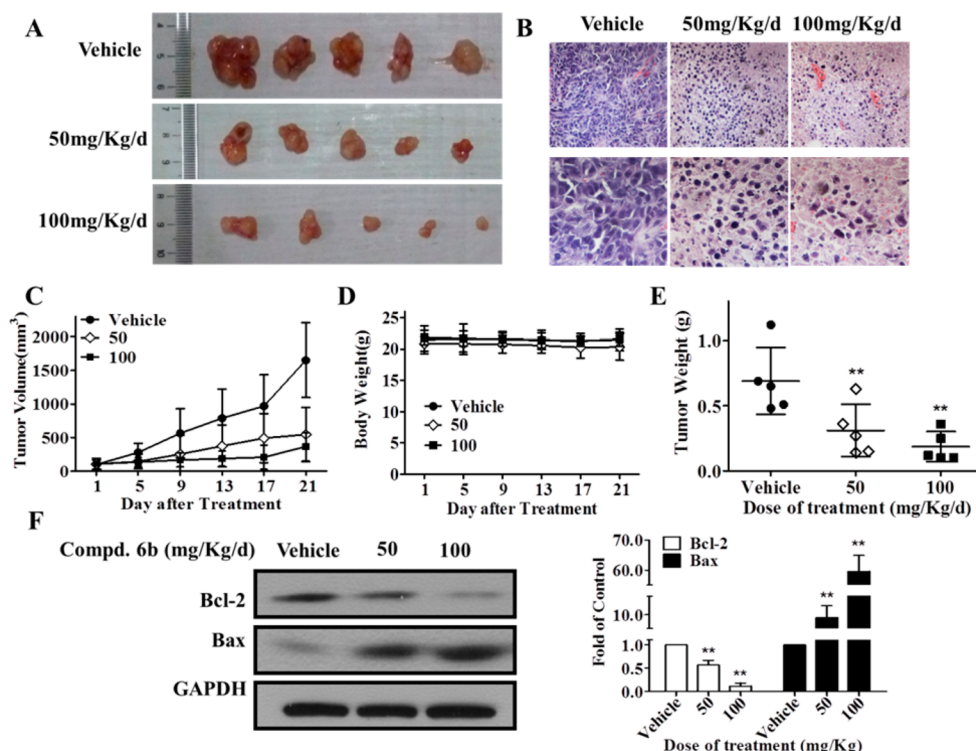


Figure 4. In vivo antitumor effects of compound 6b. (A) Represented tumors with the indicated treatment. (B) Hematoxylin and eosin (H&E) staining of the represented tumor tissues with indicated treatment. Tumor volume (C), body weight (D), and tumor weight (E) of the animal with the indicated treatment. (F) Expression level of Bcl-2 and Bax in vivo. (*) $P < 0.05$ was considered significant. (**) $P < 0.01$ was considered statistically highly significant.

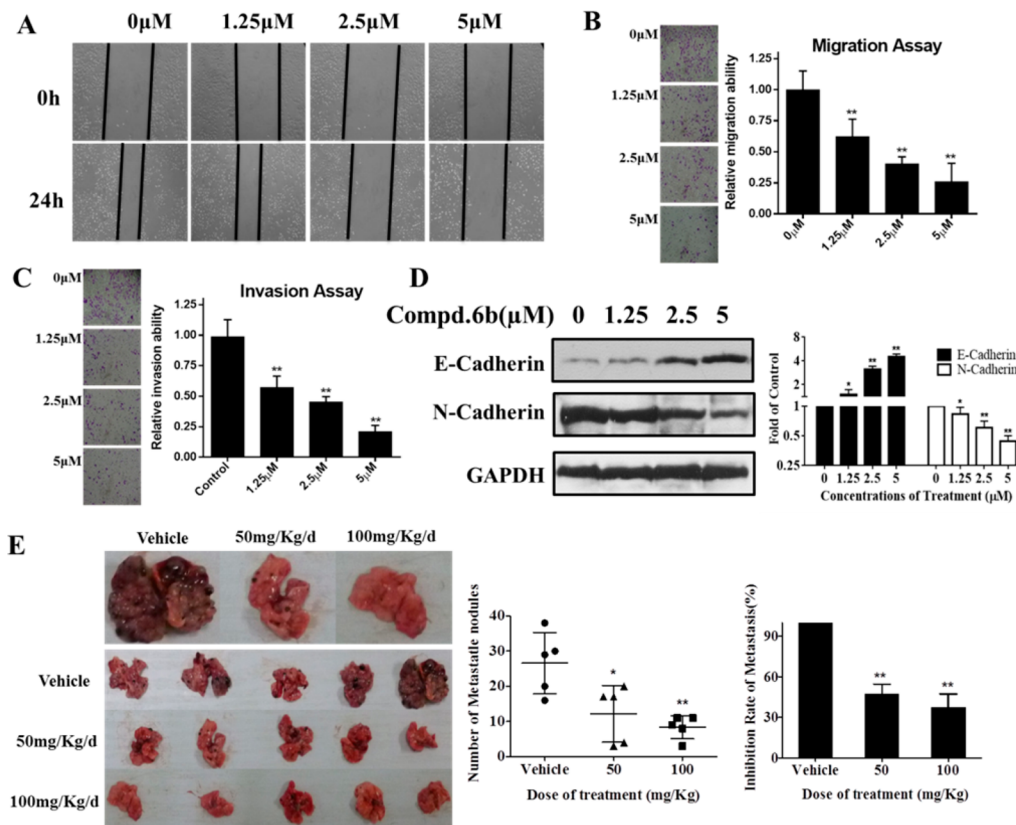


Figure 5. Compound **6b** selectively inhibited cell migration and invasion. (A) Wound healing assay. (B and C) Migration and invasion ability assay. Treatment of compound **6b** resulted in the depressed migration (B) and invasion (C) ability in MGC-803 cells. (D) Expressions of E-Cadherin and N-Cadherin after a 48 h treatment of compound **6b**. (E) Inhibitory effect of compound **6b** on lung metastasis model. (*) $P < 0.05$ was considered significant. (**) $P < 0.01$ was considered statistically highly significant.

vitro cytotoxicity of compound **6b** was evaluated by MTT method. We found that compound **6b** performed a strong cytotoxic effect on MGC-803 cells with $IC_{50} = 4.01 \pm 0.21 \mu\text{M}$ as well as on HGC-27 with $IC_{50} = 8.92 \pm 0.52 \mu\text{M}$ (Figure 3A). However, compound **6b** did not exhibit a similar effect on highly differentiated gastric cancer cell line SGC-7901 ($IC_{50} = 67.52 \pm 5.43 \mu\text{M}$) and gastric epithelial immortalized GES-1 cells ($IC_{50} = 58.91 \pm 3.41 \mu\text{M}$), respectively (Figure 3A). These findings implicate that the stronger cytotoxicity of compound **6b** on MGC-803 and HGC-27 cells may be associated with its specific target to the enhanced LSD1 in these cells.

Pro-apoptotic Effect of Compound **6b and the Involved Mechanism.** On the basis of the strong cytotoxicity of compound **6b** in MGC-803, we then determined the effect of this compound on cell apoptosis. Using Hoechst 33258 staining, characteristic apoptotic morphological changes in MGC-803 cells were observed by fluorescence microscope after 24 h incubation with compound **6b** at indicated concentrations. We found that compound **6b** treatment induced significant crescent nuclei, chromatin shrinkage, and formation of apoptotic bodies (Figure 3B). Meanwhile, Annexin V-FITC/PI double staining was also applied, and a flow cytometer was used for quantitative analysis for apoptotic cells. Our results indicate that, after 48 h treatment, compound **6b** dose dependently induced cell apoptosis (Figure 3C).

To further illustrate the mechanism of compound **6b**-induced apoptosis, the key proteins in the mitochondria-related apoptotic pathway were investigated. We found that the pro-apoptotic protein, Bax, was upregulated and the anti-apoptotic

protein, Bcl-2, was downregulated dose dependently after 48 h treatment of compound **6b** (Figure 3D). Meanwhile, siRNA-induced LSD1 knockdown was also associated with upregulated Bax and downregulated Bcl-2 (Figure 3E). Our findings indicate that LSD1 may be involved in the mitochondria-related apoptosis.

In vivo inhibitory effect of compound **6b** on tumor growth was examined in a xenograft model. Xenograft tumors were generated by subcutaneous implantation of MGC-803 cells into nude mice. After the treatment of compound **6b**, the mouse body weights were monitored and the tumor sizes were measured and recorded every 4 days (Figure 4D and E). After 21 days of treatment, compound **6b** at a dose of 50 and 100 mg/kg/d significantly delayed the growth of tumor and reduced average tumor weight by 55.1% and 72.1%, respectively, compared to the vehicle group (Figure 4A and E). There was no apparent body weight loss during the treatment, indicating the low side effects of compound **6b** in vivo (Figure 4D). Histological analysis demonstrated a dramatic change in tumor tissue, including low cell density, condensed chromatin staining, and pyknosis, indicating mitotic catastrophe and apoptosis (Figure 4B). These data indicated that compound **6b** was efficacious in inhibiting MGC-803 cells growth in vivo without obvious global toxicity. Furthermore, compound **6b** treatment in vivo also resulted in significant upregulation of Bax and downregulation of Bcl-2, similar to the findings in vitro (Figure 4F). Our results indicate that LSD1 activity inhibition in MGC-803 gastric cancer cells may be related to the mitochondrial apoptotic pathway.

Effect of Compound 6b on Cell Migration and Invasion. LSD1 was reported to regulate epithelial–mesenchymal transition (EMT), a key process for cancer cell migration and invasion, through downregulation of E-Cadherin.⁵⁹ We further evaluated the effect of compound **6b** on cell migration and invasion. Microphotographs showed that untreated MGC-803 cells filled most of the wounded area 2 days after scratching the cell monolayer, whereas treatment with indicated doses of compound **6b** markedly suppressed the wound healing (Figure 5A). Compound **6b** treatment, even below 5 μ M, also significantly inhibited the cell migration (Figure 5B) and invasion (Figure 5C) with transwell and matrigel-coated transwell experiments. These results indicated the potent migration and invasion inhibitory effects of compound **6b** in vitro. To further illustrate the mechanism of our compound on these effects, the expression levels of two biomarkers for EMT, E-Cadherin and N-Cadherin, were investigated. We found that E-Cadherin was upregulated and N-Cadherin was downregulated after compound **6b** treatment (Figure 5D), indicating the inhibitory effect of EMT by the compound.

To further investigate the in vivo inhibitory effect of compound **6b** on metastasis, B16-F10 melanoma cell was chosen to generate an in vivo artificial lung metastatic model. We found that the average number of lung metastatic nodules in the control group was 26.6 ± 8.7 ; after 50 and 100 mg/kg/day compound **6b** treatment for 14 days, this parameter was significantly reduced to 12.1 ± 8.0 and 8.4 ± 3.2 nodules, respectively (Figure 5E), indicating the significant lung metastasis inhibitory effect in vivo by compound **6b**. Our findings above suggest that LSD1 targeted compound **6b** may provide efficient inhibition of cancer cell metastasis.

CONCLUSIONS

In summary, we have designed, synthesized, and identified a novel series of pyridimine–thiourea hybrids, as potent LSD1 inhibitors to modulate cancer cell growth, migration, and invasion in vitro and in vivo. The structure–activity relationship study suggested that the most effective LSD1 inhibitor should contain both an unmodified propargyl unit and an amino-thiourea core. This work reported, for the first time, that a series of oral active pyrimidine–thiourea-based, selective LSD1 inactivators may serve as leading compounds targeting LSD1 overexpressed cancer.

METHODS

General Methods for Chemistry. Reagents and solvents were purchased from commercial sources and were used without further purification. Melting points were determined on an X-5 micromelting apparatus, and ¹H NMR and ¹³C NMR spectra were recorded on a Bruker 400 and 100 MHz spectrometer, respectively. High-resolution mass spectra were recorded on a Waters Micromass Q-T of Micromass spectrometer. The purity of all biologically evaluated compounds was determined to be >95% by reverse-phase high-performance liquid chromatography (HPLC) analysis. The signal was monitored at 274 nm with a UV detector. A flow rate of 1.0 mL/min was used with a mobile phase of MeOH in H₂O (70:30, v/v).

General Procedure for the Synthesis of Compounds 5a–j. A mixture of the appropriate 2-mercaptopidihydropyrimidine derivatives **4a–j** (1 mmol), the propargyl bromide (1 mmol), and anhydrous potassium carbonate (1 mmol) was refluxed in dry dioxane. Upon completion, as judged by thin-layer chromatography (TLC), phosphorus oxychloride was added dropwise with stirring while maintaining the temperature of the reaction mixture. Stirring was

continued for an additional 1 h. The cooled reaction mixture was poured on crushed ice, and the separated solid was filtered off, washed with water, dried, and crystallized from aqueous ethanol to yield the pure product.

4-Chloro-6-phenyl-2-(prop-2-yn-1-ylthio)pyrimidine-5-carbonitrile (5a**).** Yield 70.5%. White solid. Mp: 131–132 °C. ¹H NMR (400 MHz, CDCl₃, δ , ppm) δ 8.18–8.05 (m, 2H, Ar–H), 7.71–7.50 (m, 3H, Ar–H), 4.01 (d, J = 2.6 Hz, 2H, –CH₂–), 2.28 (t, J = 2.6 Hz, 1H, \equiv C–H). ¹³C NMR (100 MHz, CDCl₃, δ , ppm) δ 174.02, 168.73, 163.95, 134.07, 132.72, 129.35, 129.02, 114.43, 101.42, 78.17, 71.63, 20.36. HR-MS (ESI): calcd C₁₄H₉ClN₃S, [M + H]⁺ m/z, 286.0206; found, 286.0202.

4-Chloro-2-(prop-2-yn-1-ylthio)-6-(3,4,5-trimethoxyphenyl)pyrimidine-5-carbonitrile (5b**).** Yield 68.3%. White solid. Mp: 104–105 °C. ¹H NMR (400 MHz, CDCl₃, δ , ppm) δ 7.50 (s, 2H, Ar–H), 3.98 (d, J = 2.7 Hz, 2H, –CH₂–), 3.97 (s, 9H, –CH₃), 2.26 (t, J = 2.6 Hz, 1H, \equiv C–H). ¹³C NMR (100 MHz, CDCl₃, δ , ppm) δ 173.60, 167.69, 164.07, 153.33, 142.24, 128.70, 114.87, 106.98, 100.65, 78.72, 71.22, 61.08, 56.43, 20.35. HR-MS (ESI): calcd C₁₇H₁₄ClN₃NaO₃S, [M + H]⁺ m/z, 398.0342; found, 398.0340.

4-Chloro-2-(prop-2-yn-1-ylthio)-6-(p-tolyl)pyrimidine-5-carbonitrile (5c**).** Yield 65.5%. White solid. Mp: 111–112 °C. ¹H NMR (400 MHz, CDCl₃, δ , ppm) δ 8.05 (d, J = 8.2 Hz, 2H, Ar–H), 7.39 (d, J = 8.1 Hz, 2H, Ar–H), 4.01 (d, J = 2.6 Hz, 2H, –CH₂–), 2.28 (t, J = 2.6 Hz, 1H, \equiv C–H). ¹³C NMR (100 MHz, CDCl₃, δ , ppm) δ 173.79, 168.53, 163.91, 143.76, 131.30, 129.76, 114.64, 100.96, 84.11, 78.30, 71.57, 21.69, 20.32. HR-MS (ESI): calcd C₁₅H₁₁ClN₃S, [M + H]⁺ m/z, 300.0362; found, 300.0363.

4-Chloro-6-(4-isopropylphenyl)-2-(prop-2-yn-1-ylthio)pyrimidine-5-carbonitrile (5d**).** Yield 72.8%. White solid. Mp: 109–110 °C. ¹H NMR (400 MHz, CDCl₃, δ , ppm) δ 8.15–8.00 (m, 2H, Ar–H), 7.44 (m, 2H, Ar–H), 4.01 (d, J = 2.6 Hz, 2H, –CH₂–), 3.03 (hept, J = 6.9 Hz, 1H, CH), 2.28 (t, J = 2.6 Hz, 1H, \equiv C–H), 1.33 (d, J = 6.9 Hz, 6H, –CH₃). ¹³C NMR (100 MHz, CDCl₃, δ , ppm) δ 173.81, 168.55, 163.92, 131.62, 129.53, 127.21, 114.66, 100.97, 84.40, 78.06, 71.57, 34.29, 23.66, 20.31. HR-MS (ESI): calcd C₁₇H₁₅ClN₃S, [M + H]⁺ m/z, 328.0675; found, 328.0677.

4-Chloro-2-(prop-2-yn-1-ylthio)-6-(p-tolyl)pyrimidine-5-carbonitrile (5e**).** Yield 86.9%. Yellow solid. Mp: 121–122 °C. ¹H NMR (400 MHz, CDCl₃, δ , ppm) δ 8.05 (d, J = 8.2 Hz, 2H, Ar–H), 7.39 (d, J = 8.1 Hz, 2H, Ar–H), 4.01 (d, J = 2.6 Hz, 2H, –CH₂–), 2.28 (t, J = 2.6 Hz, 1H, \equiv C–H). ¹³C NMR (100 MHz, CDCl₃, δ , ppm) δ 173.79, 168.53, 163.91, 143.76, 131.30, 129.76, 114.64, 100.96, 84.11, 78.30, 71.57, 21.69, 20.32. HR-MS (ESI): calcd C₁₅H₁₁ClN₃S, [M + H]⁺ m/z, 300.0362; found, 300.0363.

4-Chloro-6-(4-nitrophenyl)-2-(prop-2-yn-1-ylthio)pyrimidine-5-carbonitrile (5f**).** Yield 65.4%. Yellow solid. Mp: 101–102 °C. ¹H NMR (400 MHz, CDCl₃, δ , ppm) δ 8.43 (d, J = 8.9 Hz, 2H, Ar–H), 8.28 (d, J = 8.9 Hz, 2H, Ar–H), 4.01 (d, J = 2.6 Hz, 2H, –CH₂–), 2.29 (t, J = 2.6 Hz, 1H, \equiv C–H). ¹³C NMR (100 MHz, CDCl₃, δ , ppm) δ 174.83, 166.55, 164.13, 149.99, 139.53, 130.51, 124.33, 124.11, 113.72, 102.07, 77.90, 71.80, 20.53. HR-MS (ESI), calcd C₁₄H₈ClN₄O₂S, [M + H]⁺ m/z, 331.0056; found, 331.0056.

4-Chloro-6-(4-chlorophenyl)-2-(prop-2-yn-1-ylthio)pyrimidine-5-carbonitrile (5g**).** Yield 77.2%. White solid. Mp: 121–122 °C. ¹H NMR (400 MHz, CDCl₃, δ , ppm) δ 8.17–8.01 (m, 2H, Ar–H), 7.63–7.47 (m, 2H, Ar–H), 4.00 (d, J = 2.6 Hz, 2H, –CH₂–), 2.28 (t, J = 2.6 Hz, 1H, \equiv C–H). ¹³C NMR (100 MHz, CDCl₃, δ , ppm) δ 174.20, 167.41, 164.04, 139.39, 132.39, 130.69, 129.40, 114.27, 101.19, 78.07, 71.66, 20.40. HR-MS (ESI): calcd C₁₄H₈Cl₂N₃S, [M + H]⁺ m/z, 319.9816; found, 319.9818.

4-Chloro-6-(3,4-difluorophenyl)-2-(prop-2-yn-1-ylthio)pyrimidine-5-carbonitrile (5h**).** Yield 82.6%. Yellow solid. Mp: 78–79 °C. ¹H NMR (400 MHz, CDCl₃, δ , ppm) δ 8.15–7.90 (m, 2H, Ar–H), 7.56–7.30 (m, 1H, Ar–H), 3.99 (t, J = 3.7 Hz, 2H, –CH₂–), 2.29 (t, J = 2.6 Hz, 1H, \equiv C–H). ¹³C NMR (100 MHz, CDCl₃, δ , ppm) δ 174.35, 166.08, 164.16, 130.83, 126.20, 119.11, 118.90, 118.20, 118.02, 114.10, 101.15, 78.07, 71.70, 20.44. HR-MS (ESI): calcd C₁₄H₇ClF₂N₃S, [M + H]⁺ m/z, 322.0017; found, 322.0013.

4-(4-Bromophenyl)-6-chloro-2-(prop-2-yn-1-ylthio)pyrimidine-5-carbonitrile (5i**).** Yield 80.5%. White solid. Mp: 137–138 °C. ¹H

NMR (400 MHz, CDCl_3 , δ , ppm) δ 8.08–7.96 (m, 2H, Ar–H), 7.84–7.60 (m, 2H, Ar–H), 4.00 (d, J = 2.6 Hz, 2H, $-\text{CH}_2-$), 2.27 (t, J = 2.6 Hz, 1H, $\equiv\text{C}-\text{H}$). ^{13}C NMR (100 MHz, CDCl_3 , δ , ppm) δ 174.24, 167.54, 164.06, 132.85, 132.39, 130.78, 127.98, 114.24, 101.19, 78.09, 71.65, 20.40. HR-MS (ESI): calcd $\text{C}_{14}\text{H}_8\text{BrClN}_3\text{S}$, [M + H]⁺ m/z , 363.9311; found, 363.9314.

General Procedure for the Synthesis of Compounds 6a–s.

To a well-stirred solution of the appropriate amine (5 mmol) in absolute ethanol (10 mL), an equimolar amount of a solution of compounds 5a–j (5 mmol) in absolute ethanol (10 mL) was added. The reaction mixture was stirred for 1.5 h at room temperature and then heated under reflux for an additional 5 h. Upon completion, the precipitated product was filtered off and washed with ethanol to afford the crude product. The crude product was recrystallized from ethanol to yield the pure product.

2-(5-Cyano-6-phenyl-2-(prop-2-yn-1-ylthio)pyrimidin-4-yl)-hydrazinecarbothioamide (6a). Yield 66.8%. Yellow solid. Mp: 213–214 °C. ^1H NMR (400 MHz, DMSO- d_6 , δ , ppm) δ 10.21 (s, 1H, pyrimidine–NH, D_2O exchangeable), 9.57 (s, 1H, thiourea–NH, D_2O exchangeable), 7.95 (d, J = 11.0 Hz, 1H, thiourea–NH₂, D_2O exchangeable), 7.91 (d, J = 6.0 Hz, 2H, Ar–H), 7.77 (s, 1H, thiourea–NH₂, D_2O exchangeable), 7.61 (t, J = 7.4 Hz, 3H, Ar–H), 4.04 (s, 2H, $-\text{CH}_2-$), 3.20 (s, 1H, $\equiv\text{C}-\text{H}$). ^{13}C NMR (100 MHz, DMSO- d_6 , δ , ppm) δ 182.71, 172.32, 167.56, 162.94, 136.04, 131.83, 129.18, 129.12, 115.60, 84.37, 80.25, 74.21, 19.63. HR-MS (ESI): calcd $\text{C}_{15}\text{H}_{13}\text{N}_6\text{S}_2$, [M + H]⁺ m/z , 341.0643; found, 341.0641.

2-(5-Cyano-2-(prop-2-yn-1-ylthio)-6-(3,4,5-trimethoxyphenyl)-pyrimidin-4-yl)hydrazinecarbothioamide (6b). Yield 80.9%. Yellow solid. Mp: 153–154 °C. ^1H NMR (400 MHz, DMSO- d_6 , δ , ppm) δ 10.15 (s, 1H, pyrimidine–NH, D_2O exchangeable), 9.57 (s, 1H, thiourea–NH, D_2O exchangeable), 7.95 (s, 1H, thiourea–NH₂, D_2O exchangeable), 7.75 (s, 1H, thiourea–NH₂, D_2O exchangeable), 7.31 (s, 2H, Ar–H), 4.02 (d, J = 2.3 Hz, 2H, $-\text{CH}_2-$), 3.86 (s, 6H, $-\text{OCH}_3$), 3.78 (s, 3H, $-\text{OCH}_3$), 3.22 (t, J = 2.5 Hz, 1H, $\equiv\text{C}-\text{H}$). ^{13}C NMR (100 MHz, DMSO- d_6 , δ , ppm) δ 182.63, 172.11, 166.67, 163.11, 153.17, 140.63, 131.00, 115.88, 106.97, 83.94, 80.74, 73.76, 60.69, 56.58, 19.77. HR-MS (ESI): calcd $\text{C}_{18}\text{H}_{18}\text{N}_6\text{NaO}_3\text{S}_2$, [M + Na]⁺ m/z , 453.0779; found, 453.0779.

2-(5-Cyano-2-(prop-2-yn-1-ylthio)-6-(*p*-tolyl)pyrimidin-4-yl)-hydrazinecarbothioamide (6c). Yield 69.1%. Yellow solid. Mp: 178–179 °C. ^1H NMR (400 MHz, DMSO- d_6 , δ , ppm) δ 10.13 (s, 1H, pyrimidine–NH, D_2O exchangeable), 9.52 (s, 1H, thiourea–NH, D_2O exchangeable), 7.92 (s, 1H, thiourea–NH₂, D_2O exchangeable), 7.80 (d, J = 7.8 Hz, 2H, Ar–H), 7.73 (s, 1H, thiourea–NH₂, D_2O exchangeable), 7.37 (d, J = 8.0 Hz, 2H, Ar–H), 4.00 (d, J = 2.5 Hz, 2H, $-\text{CH}_2-$), 3.16 (t, J = 2.6 Hz, 1H, $\equiv\text{C}-\text{H}$), 2.39 (s, 3H). ^{13}C NMR (100 MHz, DMSO- d_6 , δ , ppm) δ 182.71, 175.33, 172.16, 163.06, 142.04, 133.23, 129.68, 129.18, 115.73, 83.93, 80.28, 74.18, 21.52, 19.60. HR-MS (ESI): calcd $\text{C}_{16}\text{H}_{14}\text{N}_6\text{NaS}_2$, [M + Na]⁺ m/z , 377.0619; found, 377.0621.

2-(5-Cyano-6-(4-isopropylphenyl)-2-(prop-2-yn-1-ylthio)pyrimidin-4-yl)hydrazinecarbothioamide (6d). Yield 72.3%. Yellow solid. Mp: 191–192 °C. ^1H NMR (400 MHz, DMSO- d_6 , δ , ppm) δ 10.15 (s, 1H, pyrimidine–NH, D_2O exchangeable), 9.53 (s, 1H, thiourea–NH, D_2O exchangeable), 7.96 (s, 1H, thiourea–NH₂, D_2O exchangeable), 7.87 (d, J = 7.9 Hz, 2H, Ar–H), 7.75 (s, 1H, thiourea–NH₂, D_2O exchangeable), 7.47 (d, J = 8.1 Hz, 2H, Ar–H), 4.03 (d, J = 2.4 Hz, 2H, $-\text{CH}_2-$), 3.19 (t, J = 2.5 Hz, 1H, $\equiv\text{C}-\text{H}$), 3.00 (dt, J = 13.9, 6.9 Hz, 1H, CH), 1.27 (d, J = 6.9 Hz, 6H, CH_3). ^{13}C NMR (100 MHz, DMSO- d_6 , δ , ppm) δ 188.67, 176.31, 169.69, 161.63, 137.70, 133.70, 129.33, 127.10, 115.71, 85.74, 80.31, 74.16, 33.90, 24.07, 19.59. HR-MS (ESI): calcd $\text{C}_{18}\text{H}_{19}\text{N}_6\text{S}_2$, [M + H]⁺ m/z , 383.1113; found, 383.1117.

2-(5-Cyano-6-(4-fluorophenyl)-2-(prop-2-yn-1-ylthio)pyrimidin-4-yl)hydrazinecarbothioamide (6e). Yield 73.4%. Yellow solid. Mp: 198–199 °C. ^1H NMR (400 MHz, DMSO- d_6 , δ , ppm) δ 10.23 (s, 1H, pyrimidine–NH, D_2O exchangeable), 9.58 (s, 1H, thiourea–NH, D_2O exchangeable), 8.01 (s, 1H, thiourea–NH₂, D_2O exchangeable), 7.98 (d, J = 5.5 Hz, 2H, Ar–H), 7.75 (s, 1H, thiourea–NH, D_2O exchangeable), 7.44 (t, J = 8.8 Hz, 2H, Ar–H), 4.03 (d, J = 2.5 Hz,

2H, $-\text{CH}_2-$), 3.19 (t, J = 2.6 Hz, 1H, $\equiv\text{C}-\text{H}$). ^{13}C NMR (100 MHz, DMSO- d_6 , δ , ppm) δ 182.66, 172.30, 165.57, 163.09, 132.48, 131.77, 116.37, 115.58, 112.98, 84.20, 80.23, 74.22, 19.63. HR-MS (ESI): calcd $\text{C}_{15}\text{H}_{12}\text{FN}_6\text{S}_2$, [M + H]⁺ m/z , 359.0549; found, 359.0551.

2-(5-Cyano-6-(4-nitrophenyl)-2-(prop-2-yn-1-ylthio)pyrimidin-4-yl)hydrazinecarbothioamide (6f). Yield 69.5%. Yellow solid. Mp: 152–153 °C. ^1H NMR (400 MHz, DMSO- d_6 , δ , ppm) δ 10.38 (s, 1H, pyrimidine–NH, D_2O exchangeable), 9.65 (s, 1H, thiourea–NH, D_2O exchangeable), 8.43 (d, J = 8.4 Hz, 2H, Ar–H), 8.13 (d, J = 7.0 Hz, 2H, Ar–H), 8.01 (s, 1H, thiourea–NH₂, D_2O exchangeable), 7.76 (s, 1H, thiourea–NH₂, D_2O exchangeable), 4.04 (s, 2H, $-\text{CH}_2-$), 3.22 (s, 1H, $\equiv\text{C}-\text{H}$). ^{13}C NMR (100 MHz, DMSO- d_6 , δ , ppm) δ 180.60, 172.70, 168.33, 165.85, 149.41, 141.86, 130.69, 124.27, 115.04, 85.22, 80.06, 74.35, 19.70. HR-MS (ESI): calcd $\text{C}_{15}\text{H}_{12}\text{N}_7\text{O}_2\text{S}_2$, [M + H]⁺ m/z , 386.0494; found, 386.0497.

4-(4-Chlorophenyl)-2-(prop-2-yn-1-ylthio)-6-((3-trifluoromethyl)phenyl)amino)pyrimidine-5-carbonitrile (6g). Yield 76.2%. Yellow solid. Mp: 191–192 °C. ^1H NMR (400 MHz, DMSO- d_6 , δ , ppm) δ 10.25 (s, 1H, pyrimidine–NH, D_2O exchangeable), 9.58 (s, 1H, thiourea–NH, D_2O exchangeable), 8.15–7.71 (m, 4H, Ar–H), 7.68 (d, J = 8.5 Hz, 2H, thiourea–NH₂, D_2O exchangeable), 4.03 (d, J = 2.5 Hz, 2H, $-\text{CH}_2-$), 3.19 (t, J = 2.6 Hz, 1H, $\equiv\text{C}-\text{H}$). ^{13}C NMR (100 MHz, DMSO- d_6 , δ , ppm) δ 182.62, 172.32, 166.31, 162.69, 136.77, 134.79, 131.04, 129.29, 115.45, 84.07, 80.17, 74.27, 19.64. HR-MS (ESI): calcd $\text{C}_{15}\text{H}_{12}\text{ClN}_6\text{S}_2$, [M + H]⁺ m/z , 375.0253; found, 375.0256.

2-(5-Cyano-6-(3,4-difluorophenyl)-2-(prop-2-yn-1-ylthio)pyrimidin-4-yl)hydrazinecarbothioamide (6h). Yield 60.9%. Yellow solid. Mp: 186–187 °C. ^1H NMR (400 MHz, DMSO- d_6 , δ , ppm) δ 10.28 (s, 1H, pyrimidine–NH, D_2O exchangeable), 9.60 (s, 1H, thiourea–NH, D_2O exchangeable), 7.97 (s, 2H, thiourea–NH₂, D_2O exchangeable), 7.87–7.60 (m, 3H, Ar–H), 4.04 (d, J = 2.5 Hz, 2H, $-\text{CH}_2-$), 3.21 (t, J = 2.6 Hz, 1H, $\equiv\text{C}-\text{H}$). ^{13}C NMR (100 MHz, DMSO- d_6 , δ , ppm) δ 182.63, 172.47, 165.02, 162.85, 153.09, 148.60, 141.22, 133.43, 126.68, 118.61, 115.35, 84.67, 80.25, 74.22, 19.69. HR-MS (ESI): calcd $\text{C}_{15}\text{H}_{10}\text{F}_2\text{N}_6\text{NaS}_2$, [M + Na]⁺ m/z , 399.0274; found, 399.0276.

2-(6-(4-Bromophenyl)-5-cyano-2-(prop-2-yn-1-ylthio)pyrimidin-4-yl)hydrazinecarbothioamide (6i). Yield 56.9%. Yellow solid. Mp: 185–186 °C. ^1H NMR (400 MHz, DMSO- d_6 , δ , ppm) δ 10.26 (s, 1H, pyrimidine–NH, D_2O exchangeable), 9.58 (s, 1H, thiourea–NH, D_2O exchangeable), 8.64 (s, 2H, thiourea–NH₂, D_2O exchangeable), 8.01–7.47 (m, 4H, Ar–H), 4.03 (d, J = 2.5 Hz, 2H, $-\text{CH}_2-$), 3.19 (t, J = 2.6 Hz, 1H, $\equiv\text{C}-\text{H}$). ^{13}C NMR (100 MHz, DMSO- d_6 , δ , ppm) δ 181.73, 172.33, 166.99, 162.69, 135.16, 132.22, 131.19, 125.66, 115.46, 84.09, 80.18, 74.26, 19.64. HR-MS (ESI): calcd $\text{C}_{15}\text{H}_{11}\text{BrN}_6\text{NaS}_2$, [M + Na]⁺ m/z , 440.9568; found, 440.9555.

2-(6-(4-Chlorophenyl)-5-cyano-2-(prop-2-yn-1-ylthio)pyrimidin-4-yl)hydrazinecarboxamide (6l). Yield 67.3%. Yellow solid. Mp: 159–160 °C. ^1H NMR (400 MHz, DMSO- d_6 , δ , ppm) δ 10.25 (s, 1H, pyrimidine–NH, D_2O exchangeable), 9.58 (s, 1H, urea–NH, D_2O exchangeable), 7.95 (s, 1H, urea–NH₂, D_2O exchangeable), 7.93 (d, J = 8.1 Hz, 2H, Ar–H), 7.74 (s, 1H, urea–NH₂, D_2O exchangeable), 7.68 (d, J = 8.5 Hz, 2H, Ar–H), 4.03 (d, J = 2.5 Hz, 2H, $-\text{CH}_2-$), 3.19 (t, J = 2.6 Hz, 1H, $\equiv\text{C}-\text{H}$). ^{13}C NMR (100 MHz, DMSO- d_6 , δ , ppm) δ 182.68, 172.40, 166.67, 162.87, 136.78, 134.80, 131.04, 129.29, 115.45, 84.39, 80.17, 74.27, 19.64. HR-MS (ESI): calcd $\text{C}_{15}\text{H}_{12}\text{ClN}_6\text{OS}$, [M + H]⁺ m/z , 359.0482; found, 359.0485.

2-(5-Cyano-6-(3,4-difluorophenyl)-2-(prop-2-yn-1-ylthio)pyrimidin-4-yl)hydrazinecarboxamide (6m). Yield 76.5%. Yellow solid. Mp: 186–187 °C. ^1H NMR (400 MHz, DMSO- d_6 , δ , ppm) δ 9.94 (s, 1H, pyrimidine–NH, D_2O exchangeable), 8.14 (s, 1H, urea–NH, D_2O exchangeable), 8.03–7.63 (m, 3H, Ar–H), 6.14 (s, 2H, urea–NH₂, D_2O exchangeable), 4.02 (d, J = 2.4 Hz, 2H, $-\text{CH}_2-$), 3.21 (t, J = 2.5 Hz, 1H, $\equiv\text{C}-\text{H}$). ^{13}C NMR (100 MHz, DMSO- d_6 , δ , ppm) δ 179.64, 175.66, 172.63, 163.32, 148.70, 133.71, 126.78, 123.15, 118.84, 118.35, 115.72, 83.70, 80.26, 74.18, 19.58. HR-MS (ESI): calcd $\text{C}_{15}\text{H}_{10}\text{F}_2\text{N}_6\text{NaOS}$, [M + Na]⁺ m/z , 383.0503; found, 383.0504.

2-(5-Cyano-2-(prop-2-yn-1-ylthio)-6-(*p*-tolyl)pyrimidin-4-yl)hydrazinecarboxamide (6n). Yield 65.6%. Yellow solid. Mp: 193–

194 °C. ^1H NMR (400 MHz, DMSO- d_6 , δ , ppm) δ 9.96 (s, 1H, pyrimidine-NH, D₂O exchangeable), 8.22 (s, 1H, urea-NH, D₂O exchangeable), 7.67 (m, 4H, Ar-H), 6.20 (d, J = 47.3 Hz, 2H, urea-NH₂, D₂O exchangeable), 4.08 (d, J = 54.9 Hz, 2H, -CH₂-), 3.33 (s, 1H, ≡C-H), 2.51 (s, 1H, -CH₃). ^{13}C NMR (100 MHz, DMSO- d_6 , δ , ppm) δ 186.63, 172.33, 167.66, 163.67, 141.68, 129.59, 129.23, 115.99, 109.68, 86.04, 80.38, 74.13, 21.51, 19.48. HR-MS (ESI): calcd C₁₆H₁₅N₆OS, [M + H]⁺ m/z , 339.1028; found, 339.1029.

2-(5-Cyano-6-(4-isopropylphenyl)-2-(prop-2-yn-1-ylthio)pyrimidin-4-yl)hydrazinecarboxamide (6o). Yield 66.5%. Yellow solid. Mp: 178–179 °C. ^1H NMR (400 MHz, DMSO- d_6 , δ , ppm) δ 9.84 (s, 1H, pyrimidine-NH, D₂O exchangeable), 8.11 (s, 1H, thiourea-NH, D₂O exchangeable), 7.85 (s, 2H, Ar-H), 7.45 (d, J = 7.8 Hz, 2H, Ar-H), 6.16 (s, 2H, thiourea-NH₂, D₂O exchangeable), 4.01 (d, J = 2.4 Hz, 2H, -CH₂-), 3.20 (t, J = 2.5 Hz, 1H), 2.99 (dt, J = 13.7, 6.8 Hz, 1H, ≡C-H), 1.26 (d, J = 6.9 Hz, 6H). ^{13}C NMR (100 MHz, DMSO- d_6 , δ , ppm) δ 172.28, 167.48, 159.10, 152.51, 133.74, 129.36, 127.00, 115.99, 82.99, 80.37, 74.09, 33.90, 24.07, 19.46. HR-MS (ESI), calcd C₁₈H₁₉N₆OS, [M + H]⁺ m/z , 367.1341; found, 367.1343.

2-(6-(3-Chlorophenyl)-5-cyano-2-(prop-2-yn-1-ylthio)pyrimidin-4-yl)hydrazinecarboxamide (6p). Yield 65.2%. Yellow solid. Mp: 187–188 °C. ^1H NMR (400 MHz, DMSO- d_6 , δ , ppm) δ 9.91 (s, 1H, pyrimidine-NH, D₂O exchangeable), 8.11 (s, 1H, urea-NH, D₂O exchangeable), 7.93–7.53 (m, 4H, Ar-H), 6.12 (s, 2H, urea-NH₂, D₂O exchangeable), 3.99 (d, J = 2.5 Hz, 2H, -CH₂-), 3.18 (t, J = 2.5 Hz, 1H, ≡C-H). ^{13}C NMR (100 MHz, DMSO- d_6 , δ , ppm) δ 186.02, 176.32, 166.01, 163.38, 138.08, 133.77, 131.52, 131.02, 128.96, 127.89, 115.45, 83.41, 80.27, 74.18, 19.56. HR-MS (ESI): calcd C₁₅H₁₁ClN₆NaOS, [M + Na]⁺ m/z , 381.0301; found, 381.0301.

2-(5-Cyano-6-(4-nitrophenyl)-2-(prop-2-yn-1-ylthio)pyrimidin-4-yl)hydrazinecarboxamide (6q). Yield 66.9%. Yellow solid. Mp: 193–194 °C. ^1H NMR (400 MHz, DMSO- d_6 , δ , ppm) δ 10.03 (s, 1H, pyrimidine-NH, D₂O exchangeable), 8.42 (s, 1H, urea-NH, D₂O exchangeable), 8.40 (s, 1H, Ar-H), 8.15 (s, 3H, Ar-H), 6.16 (s, 2H, urea-NH₂, D₂O exchangeable), 4.03 (d, J = 2.3 Hz, 2H, -CH₂-), 3.20 (t, J = 2.6 Hz, 1H, ≡C-H). ^{13}C NMR (100 MHz, DMSO- d_6 , δ , ppm) δ 172.69, 165.70, 163.22, 159.16, 149.35, 141.96, 130.75, 124.19, 115.21, 84.38, 80.05, 74.32, 19.59. HR-MS (ESI): calcd C₁₅H₁₂N₇O₃S, [M + H]⁺ m/z , 370.0722; found, 370.0723.

2-(6-(4-Bromophenyl)-5-cyano-2-(prop-2-yn-1-ylthio)pyrimidin-4-yl)hydrazinecarboxamide (6r). Yield 69.5%. Yellow solid. Mp: 178–179 °C. ^1H NMR (400 MHz, DMSO- d_6 , δ , ppm) δ 9.92 (s, 1H, pyrimidine-NH, D₂O exchangeable), 8.13 (s, 1H, urea-NH, D₂O exchangeable), 7.82 (m, 4H, Ar-H), 6.15 (s, 2H, urea-NH₂, D₂O exchangeable), 4.02 (d, J = 2.4 Hz, 2H, -CH₂-), 3.19 (t, J = 2.5 Hz, 1H, ≡C-H). ^{13}C NMR (100 MHz, DMSO- d_6 , δ , ppm) δ 187.68, 179.33, 169.31, 163.44, 135.25, 132.14, 131.26, 125.59, 115.58, 83.40, 80.21, 74.22, 19.50. HR-MS (ESI): calcd C₁₅H₁₁BrN₆NaOS, [M + Na]⁺ m/z , 424.9796; found, 424.9798.

2-(5-Cyano-6-(4-nitrophenyl)-2-(prop-2-yn-1-ylthio)pyrimidin-4-yl)hydrazinecarboximidamide (6s). Yield 66.1%. Yellow solid. Mp: 178–179 °C. ^1H NMR (400 MHz, DMSO- d_6 , δ , ppm) δ 12.82 (s, 1H, NH, D₂O exchangeable), 8.64–8.27 (m, 2H, Ar-H), 8.12 (m, 2H, Ar-H), 5.25 (s, 2H, guanidine-NH₂, D₂O exchangeable), 4.05 (d, J = 2.5 Hz, 2H, -CH₂-), 3.16 (t, J = 2.5 Hz, 1H, ≡C-H). ^{13}C NMR (100 MHz, DMSO- d_6 , δ , ppm) δ 186.63, 174.36, 166.47, 161.34, 149.05, 142.73, 131.18, 124.27, 115.70, 84.09, 80.88, 73.68, 19.25. HR-MS (ESI): calcd C₁₅H₁₃N₈O₂S, [M + H]⁺ m/z , 369.0882; found, 369.0880.

Cells and Cell Viability Assay. The human gastric carcinoma cell lines MGC-803 and HGC-27 were supplied by the Cell Bank of Shanghai Institute of Cell Biology, Chinese Academy of Sciences. Human gastric carcinoma cell line SGC-7901 was purchased from Shanghai Bogoo Biotechnology Company. Human gastric epithelial mucosa cell line GES-1 was preserved in our institute. Cells were cultured in Dulbecco's modified Eagle's medium (DMEM) or RPMI-1640 medium. All media was supplemented with 10% fetal bovine serum (FBS). Cells were cultured in an incubator with 5% CO₂ at 37 °C in a humidified atmosphere.

The cell viability was determined by 3-(4,5-dimethylthiazol-2-yl)-2,5-diphenyltetrazolium bromide (MTT) assay with 72 h indicated treatment and colony formation after 10-day treatment using a clonogenic survival assay. The data were analyzed with SPSS 20.

Inhibitory Evaluation of the Candidate Compounds against LSD1, MAO-A, and MAO-B and Mechanism of Action Studies. Inhibitory effects of the candidate compounds against LSD1, MAO-A, and MAO-B were evaluated as previously published.⁵⁸ Briefly, cDNA encoding LSD1(157–852AA) was obtained by reverse transcription polymerase chain reaction (RT-PCR) and cloned into pET28b to have the constructed plasmid pET28b-LSD1, and then the plasmid was transfected into BL21(DE). The recombinant was induced with 0.25 mM isopropyl β-D-1-thiogalactopyranoside (IPTG) at 20 °C and purified with Ni-NTA (NTA = nitrilotriacetic acid) resin. Then the compounds were incubated with the recombinant and H3K4me2, and after that, the fluorescence was measured at an excitation wavelength of 530 nm and an emission wavelength of 590 nm with the addition of Amplex Red and horseradish peroxidase (HRP) in order to evaluate the inhibition rate of the candidate compound. Inhibitory effects of the candidate compounds against MAO-A and MAO-B were evaluated with enzyme from Sigma and a commercialized kit from Promega.

BLI Assay. The direct interaction between small molecules and LSD1 was quantified using BLI Octet RED96 (FortéBio Inc., Menlo Park, CA). The protein LSD1 was biotinylated using NHS-LCLC-biotin (cat. no. 21343, Pierce) at a molar coupling ratio (MCR) of 1:1 under room temperature for 1 h; then the reaction was stopped by removing the excess biotin reagent using the desalting column (cat. no. 89883, Thermo), and the concentration of biotinylated protein was adjusted to 30 μg/mL. Superstreptavidin biosensors (FortéBio Inc.) were coated in a solution containing 30 μg/mL of biotinylated protein for 5 min at 30 °C. A duplicate set of sensors was incubated in an assay buffer (50 mM 4-(2-hydroxyethyl)-1-piperazineethanesulfonic acid (HEPES) pH 8.0 and 1% dimethylsulfoxide (DMSO)) without protein for use as a background binding control. Both sets of sensors were then blocked with a solution of 5 μM biocytin (EZ-Link Biocytin, cat. no. 28022, Thermo) for 60 s at 30 °C. Binding of samples (100, 50, 25, 12.5, 6.25, and 3.125 μM) to coated and uncoated reference sensors was measured over 60 s. Data analysis on the FortéBio Octet RED96 instrument was performed using a double reference subtraction (sample and sensor references) in the FortéBio data analysis software, which accounts for nonspecific binding, background, and signal drift and minimizes well-based and sensor variability, while K_d values were fitted using a 1:1 model.

Migration and Invasion Assay. Cell migration and invasion ability were evaluated by wound healing assay, transwell assay, and matrigel-coated transwell assay. All these experiments were carried out as previously published.⁵⁸

Briefly, for the wound-healing assay, cells were placed in a 24-well plate, and the cell surface was scratched using a 10 μL pipet tip. Then cells were treated with compound 6b with different concentrations followed by 48 h incubation and photographed on an inverted microscope.

For migration assays, cells were plated in Transwell 24-well plates. Heat-inactivated FBS (1%) and 20% FBS were supplemented into upper and lower chambers separately. Different concentrations of the candidate compound were added in the chamber. After 48 h, the medium was removed and the chambers were washed. Noninvasive cells were removed from the upper surface of the membrane by scrubbing with a cotton-tipped swab, and the invasive cells were fixed with methanol for 15 min. Then the chambers were stained with crystal violet. Six fields for each chamber were photographed on an inverted microscope, and invasive cells were counted in each field.

For the invasion assay, cells were plated in Transwell 24-well plates with Matrigel. The medium, attractant, staining, and cell counting method were the same as those of the transwell assay.

Apoptotic Analysis. Changes of cell nucleus morphology were observed by Hoechst-33258 staining. Cells were treated with compound 6b at the indicated concentrations for 48 h and harvested by trypsinization followed by being fixed with 4% paraformaldehyde and incubated with 0.5% Triton X-100; cells were then stained with 5

$\mu\text{g/mL}$ Hoechst-33258 in phosphate-buffered saline (PBS) in the dark for 20 min. After being washed twice, apoptosis cells were examined and identified according to the condensation and fragmentation of nuclei by fluorescence microscopy under UV excitation.

The apoptosis was quantified by BD Accuri C6 flow cytometer (Becton Dickinson) with AnnexinV-FITC/PI staining kit from Roche. Ten thousand events for each sample were counted and analyzed. The early and late apoptotic cells were identified by the fluorescence intensity of fluorescein isothiocyanate (FITC) and propidium iodide (PI).

SiRNA Transfection. Cells (6×10^5) were seeded in a 6-well plate and then incubated for 2 days in standard medium in the presence of 20–100 nM siRNA directed against LSD1 or control siRNA (scrambled) complexed with Lipofectamine RNAiMAX reagent according to the manufacturer's instructions.

Western Blot. Western blot was performed with the total lysates by radio-immunoprecipitation assay (RIPA) or histone purified with a kit from Epigentek. Equal amounts of cell lysates were denatured, separated by sodium dodecyl sulfate polyacrylamide gel electrophoresis (SDS-PAGE), and transferred to 0.2 μM nitrocellulose membranes. After blocking with PBS containing 5% nonfat milk, the membranes were incubated overnight at 4 °C with primary antibody, followed by incubation with a horseradish peroxidase-conjugated secondary antibody. The immunoblots were visualized by enhanced chemiluminescence kit from Thermo Fisher.

Antibodies used were against histone H3K4me (Selleck Chemicals no. A1237), H3K4me2 (Epitomics no. 1347-1), H3K9me2 (Epitomics no. 1349-1), H3K4me3 (Bioss, bs-4715R), total H3 (Sino Biological Inc. no. 100005-MM01), total H4 (EnoGene no. E1A635S), LSD1 (Epitomics no. 5890-1), E-Cadherin (Epitomics no. 1702-1), N-Cadherin (Cell Signaling no. 3879), Bax (Epitomics, no. 1063-1), Bcl-2 (Epitomics, no. 1017-1), and glyceraldehyde 3-phosphate dehydrogenase (GAPDH) (GoodHere no. AB-M-M 001).

Animal Studies. Xenograft models using human gastric cancer cell line (MGC-803) were established in BALB/C mice. Once the volume of tumors reached 100 mm^3 , mice were divided into control groups and treatment groups. The treatment groups received compound **6b** (50, 100 mg/kg, p.o.) per day for a period of 21 days. Tumor volumes were measured at 3-day intervals. After the 21st day, the mice were euthanized and the tumors were isolated, weighed, and then stored at –85 °C or fixed in 4% paraformaldehyde followed by being embedded in paraffin. Tumor size was determined by caliper measurements, and the body weight was measured at 4-day intervals to monitor drug toxicity.

Male C57BL/6 mice (6–8 weeks old) weighing 20–25 g were maintained in a temperature- and humidity-controlled environment with a 12-h/12-h light/dark cycle. B16-F10 melanoma cells were collected to an appropriate concentration in PBS and injected via tail vein into syngeneic C57BL/6 mice from Shanghai Laboratory Animal Center (Shanghai, China). The mice were equally randomized into three groups (5 mice/group): control group, compound **6b** 50 mg/kg/day, and compound **6b** 100 mg/kg/day group. The compound was administrated orally for 14 days. Then the mice were weighed and sacrificed. The lungs were removed and washed with PBS. The number of metastasis nodules on the lung surface was counted under a dissecting microscope.

Histological Analysis. The histologies of paraffin-embedded tumor sections were analyzed by hematoxylin and eosin (H&E) staining.

Statistical Analyses. Data were expressed as the mean \pm SD. The significance of the difference between different groups was determined with analysis of variance (ANOVA) and Student *t* test. Results were considered statistically significant at $P < 0.05$. $P < 0.01$ was considered highly significant.

ASSOCIATED CONTENT

Supporting Information

Characterization data for selected compounds. This material is available free of charge via the Internet at <http://pubs.acs.org>.

AUTHOR INFORMATION

Corresponding Authors

*E-mail: zhaowen100@139.com.

*E-mail: liuhm@zzu.edu.cn. Phone: 86-371-67781739.

Author Contributions

[†]L.-Y.M, Y.-C.Z., and S.-Q.W. contributed equally.

Notes

The authors declare no competing financial interest.

ACKNOWLEDGMENTS

This work was supported by National Natural Science Foundation of China (Project nos. 81430085, 21372206, and 81172937 for H.-M.L.; Project nos. 81270270 and 81470524 for W.Z.); Ph.D Educational Award from Ministry of Education (no. 20134101130001 for H.-M.L. and no. 20134101110013 for W.Z.); The 2013 Scientific Innovation Talent Award from Department of Education of Henan Province (no. 13HAS-TIT029 for W.Z.); The 2013 Young Teacher Foundation from Zhengzhou University (No. 000001307615 for Y.-C. Z.). We are grateful to Dr. Shaomin Wang, Analysis and Testing Center, Zhengzhou University, for performing the HR-ESI-MS experiments and Bing Zhao, School of Pharmaceutical Sciences, Zhengzhou University, for the NMR analysis.

REFERENCES

- (1) Shi, Y.; Lan, F.; Matson, C.; Mulligan, P.; Whetstone, J. R.; Cole, P. A.; Casero, R. A.; Shi, Y. Histone Demethylation Mediated by the Nuclear Amine Oxidase Homolog LSD1. *Cell* **2004**, *119*, 941–953.
- (2) Lynch, J. T.; Harris, W. J.; Somerville, T. C. P. LSD1 inhibition: A therapeutic strategy in cancer? *Expert Opin. Ther. Targets* **2012**, *16*, 1239–1249.
- (3) Suzuki, T.; Miyata, N. Lysine Demethylases Inhibitors. *J. Med. Chem.* **2011**, *54*, 8236–8250.
- (4) Lee, M. G.; Wynder, C.; Schmidt, D. M.; McCafferty, D. G.; Shiekhattar, R. Histone H3 Lysine 4 Demethylation Is a Target of Nonselective Antidepressive Medications. *Chem. Biol.* **2006**, *13*, 563–567.
- (5) Wang, J.; Lu, F.; Ren, Q.; Sun, H.; Xu, Z.; Lan, R.; Liu, Y.; Ward, D.; Quan, J.; Ye, T.; Zhang, H. Novel Histone Demethylase LSD1 Inhibitors Selectively Target Cancer Cells with Pluripotent Stem Cell Properties. *Cancer Res.* **2011**, *71*, 7238–7249.
- (6) Hitchin, J. R.; Blagg, J.; Burke, R.; Burns, S.; Cockerill, M. J.; Fairweather, E. E.; Hutton, C.; Jordan, A. M.; McAndrew, C.; Mirza, A.; Mould, D.; Thomson, G. J.; Waddell, I.; Ogilvie, D. J. Development and evaluation of selective, reversible LSD1 inhibitors derived from fragments. *Med. Chem. Commun.* **2013**, *4*, 1513–1522.
- (7) Dulla, B.; Kirla, K. T.; Rathore, V.; Deora, G. S.; Kavela, S.; Maddika, S.; Chatti, K.; Reiser, O.; Iqbal, J.; Pal, M. Synthesis and evaluation of 3-amino/guanidine substituted phenyl oxazoles as a novel class of LSD1 inhibitors with anti-proliferative properties. *Org. Biomol. Chem.* **2013**, *11*, 3103–3107.
- (8) Itoh, Y.; Suzuki, T.; Miyata, N. Small-molecular modulators of cancer-associated epigenetic mechanisms. *Mol. Biosyst.* **2013**, *9*, 873–896.
- (9) Sorna, V.; Theisen, E. R.; Stephens, B.; Warner, S. L.; Bearss, D. J.; Vankayalapati, H.; Sharma, S. High-Throughput Virtual Screening Identifies Novel *N'*-(1-Phenylethylidene)-benzohydrazides as Potent, Specific, and Reversible LSD1 Inhibitors. *J. Med. Chem.* **2013**, *56*, 9496–9508.
- (10) Prusevich, P.; Kalin, J. H.; Ming, S. A.; Basso, M.; Givens, J.; Li, X.; Hu, J.; Taylor, M. S.; Cieniewicz, A. M.; Hsiao, P.-Y.; Huang, R.; Roberson, H.; Adejola, N.; Avery, L. B.; Casero, R. A.; Taverna, S. D.; Qian, J.; Tackett, A. J.; Ratan, R. R.; McDonald, O. G.; Feinberg, A. P.; Cole, P. A. A Selective Phenelzine Analogue Inhibitor of Histone Demethylase LSD1. *ACS Chem. Biol.* **2014**, *9*, 1284–1293.

- (11) Ye, X.-W.; Zheng, Y.; Duan, Y.-C.; Wang, M.-M.; Yu, B.; Ren, J.-L.; Ma, J.-L.; Zhang, E.; Liu, H.-M. Synthesis and biological evaluation of coumarin-1,2,3-triazole-dithiocarbamate hybrids as potent LSD1 inhibitors. *Med. Chem. Commun.* **2014**, *5*, 650–654.
- (12) Willmann, D.; Lim, S.; Wetzel, S.; Metzger, E.; Jandausch, A.; Wilk, W.; Jung, M.; Forne, I.; Imhof, A.; Janzer, A.; Kifel, J.; Waldmann, H.; Schüle, R.; Buettner, R. Impairment of prostate cancer cell growth by a selective and reversible lysine-specific demethylase 1 inhibitor. *Int. J. Cancer* **2012**, *131*, 2704.
- (13) Tortorici, M.; Borrello, M. T.; Tardugno, M.; Chiarelli, L. R.; Pilotto, S.; Ciossani, G.; Vellore, N. A.; Bailey, S. G.; Cowan, J.; O'Connell, M.; Crabb, S. J.; Packham, G.; Mai, A.; Baron, R.; Ganesan, A.; Mattevi, A. Protein Recognition by Short Peptide Reversible Inhibitors of the Chromatin-Modifying LSD1/CoREST Lysine Demethylase. *ACS Chem. Biol.* **2013**, *8*, 1677.
- (14) Sharma, M.; Chauhan, K.; Shivahare, R.; Vishwakarma, P.; Suthar, M. K.; Sharma, A.; Gupta, S.; Saxena, J. K.; Lal, J.; Chandra, P.; Kumar, B.; Chauhan, P. M. S. Discovery of a New Class of Natural Product-Inspired Quinazolinone Hybrid as Potent Antileishmanial Agents. *J. Med. Chem.* **2013**, *56*, 4374–4392.
- (15) Parveen, H.; Hayat, F.; Salahuddin, A.; Azam, A. Synthesis, characterization and biological evaluation of novel 6-ferrocenyl-4-aryl-2-substituted pyrimidine derivatives. *Eur. J. Med. Chem.* **2010**, *45*, 3497–3503.
- (16) Choi, Y.; Li, L.; Grill, S.; Gullen, E.; Lee, C. S.; Gumina, G.; Tsujii, E.; Cheng, Y.-C.; Chu, C. K. Structure–Activity Relationships of (E)-5-(2-Bromovinyl)uracil and Related Pyrimidine Nucleosides as Antiviral Agents for Herpes Viruses. *J. Med. Chem.* **2000**, *43*, 2538–2546.
- (17) McGuigan, C.; Barucki, H.; Blewett, S.; Carangio, A.; Erichsen, J. T.; Andrei, G.; Snoeck, R.; De Clercq, E.; Balzarini, J. Highly Potent and Selective Inhibition of Varicella-Zoster Virus by Bicyclic Europyrimidine Nucleosides Bearing an Aryl Side Chain. *J. Med. Chem.* **2000**, *43*, 4993–4997.
- (18) Hopkins, A. L.; Ren, J.; Tanaka, H.; Baba, M.; Okamoto, M.; Stuart, D. I.; Stammers, D. K. Design of MKC-442 (Emivirine) Analogues with Improved Activity Against Drug-Resistant HIV Mutants. *J. Med. Chem.* **1999**, *42*, 4500–4505.
- (19) Pontikis, R.; Dollé, V.; Guillaumel, J.; Dechaux, E.; Note, R.; Nguyen, C. H.; Legraverend, M.; Bisagni, E.; Aubertin, A.-M.; Grierson, D. S.; Monneret, C. Synthesis and Evaluation of “AZT-HEPT”, “AZT-Pyridinone”, and “ddC-HEPT” Conjugates as Inhibitors of HIV Reverse Transcriptase1. *J. Med. Chem.* **2000**, *43*, 1927–1939.
- (20) Palanki, M. S. S.; Erdman, P. E.; Gayo-Fung, L. M.; Shevlin, G. I.; Sullivan, R. W.; Goldman, M. E.; Ransone, L. J.; Bennett, B. L.; Manning, A. M.; Suto, M. J. Inhibitors of NF- κ B and AP-1 Gene Expression: SAR Studies on the Pyrimidine Portion of 2-Chloro-4-trifluoromethylpyrimidine-5-[N-(3',5'-bis(trifluoromethyl)phenyl)-carboxamide]. *J. Med. Chem.* **2000**, *43*, 3995–4004.
- (21) Ohmoto, K.; Yamamoto, T.; Horiuchi, T.; Imanishi, H.; Odagaki, Y.; Kawabata, K.; Sekioka, T.; Hirota, Y.; Matsuoka, S.; Nakai, H.; Toda, M.; Cheronis, J. C.; Spruce, L. W.; Gyorkos, A.; Wieczorek, M. Design and Synthesis of New Orally Active Nonpeptidic Inhibitors of Human Neutrophil Elastase. *J. Med. Chem.* **2000**, *43*, 4927–4929.
- (22) Esteban-Gamboa, A.; Balzarini, J.; Esnouf, R.; De Clercq, E.; Camarasa, M.-J.; Pérez-Pérez, M.-J. Design, Synthesis, and Enzymatic Evaluation of Multisubstrate Analogue Inhibitors of *Escherichia coli* Thymidine Phosphorylase. *J. Med. Chem.* **2000**, *43*, 971–983.
- (23) Fargualy, A. M.; Habib, N. S.; Ismail, K. A.; Hassan, A. M. M.; Sarg, M. T. M. Synthesis, biological evaluation and molecular docking studies of some pyrimidine derivatives. *Eur. J. Med. Chem.* **2013**, *66*, 276–295.
- (24) Abdel-Mohsen, H. T.; Ragab, F. A. F.; Ramla, M. M.; El Diwani, H. I. Novel benzimidazole-pyrimidine conjugates as potent antitumor agents. *Eur. J. Med. Chem.* **2010**, *45*, 2336–2344.
- (25) Rostom, S. A. F.; Ashour, H. M. A.; Abd El Razik, H. A. Synthesis and Biological Evaluation of Some Novel Polysubstituted Pyrimidine Derivatives as Potential Antimicrobial and Anticancer Agents. *Arch. Pharm.* **2009**, *342*, 299–310.
- (26) Curtin, N. J.; Barlow, H. C.; Bowman, K. J.; Calvert, A. H.; Davison, R.; Golding, B. T.; Huang, B.; Loughlin, P. J.; Newell, D. R.; Smith, P. G.; Griffin, R. J. Resistance-Modifying Agents. 11. 1 Pirimido[5,4-*d*]pyrimidine Modulators of Antitumor Drug Activity. Synthesis and Structure–Activity Relationships for Nucleoside Transport Inhibition and Binding to α_1 -Acid Glycoprotein. *J. Med. Chem.* **2004**, *47*, 4905–4922.
- (27) Conejo-García, A.; García-Rubiño, M. E.; Marchal, J. A.; Núñez, M. C.; Ramírez, A.; Cimino, S.; García, M. Á.; Aránega, A.; Gallo, M. A.; Campos, J. M. Synthesis and anticancer activity of (RS)-9-(2,3-dihydro-1,4-benzoxazepin-2-ylmethyl)-9*H*-purines. *Eur. J. Med. Chem.* **2011**, *46*, 3795–3801.
- (28) López-Cara, L. C.; Conejo-García, A.; Marchal, J. A.; Macchione, G.; Cruz-López, O.; Boulaiz, H.; García, M. A.; Rodríguez-Serrano, F.; Ramírez, A.; Cativiela, C.; Jiménez, A. I.; García-Ruiz, J. M.; Choquesillo-Lazarte, D.; Aránega, A.; Campos, J. M. New (RS)-benzoxazepin-purines with antitumour activity: The chiral switch from (RS)-2,6-dichloro-9-[1-(*p*-nitrobenzenesulfonyl)-1,2,3,5-tetrahydro-4,1-benzoxazepin-3-yl]-9*H*-purine. *Eur. J. Med. Chem.* **2011**, *46*, 249–258.
- (29) Martin, D. S.; Bertino, J. R.; Koutcher, J. A. ATP Depletion + Pyrimidine Depletion Can Markedly Enhance Cancer Therapy: Fresh Insight for a New Approach. *Cancer Res.* **2000**, *60*, 6776–6783.
- (30) Morales, F.; Ramírez, A.; Conejo-García, A.; Morata, C.; Marchal, J. A.; Campos, J. M. Anti-proliferative activity of 2,6-dichloro-9- or 7-(ethoxycarbonylmethyl)-9*H*- or 7*H*-purines against several human solid tumour cell lines. *Eur. J. Med. Chem.* **2014**, *76*, 118–124.
- (31) Altomare, C.; Cellamare, S.; Summo, L.; Catto, M.; Carotti, A.; Thull, U.; Carrupt, P.-A.; Testa, B.; Stoeckli-Evans, H. Inhibition of Monoamine Oxidase-B by Condensed Pyridazines and Pyrimidines: Effects of Lipophilicity and Structure–Activity Relationships. *J. Med. Chem.* **1998**, *41*, 3812–3820.
- (32) Carotti, A.; Catto, M.; Leonetti, F.; Campagna, F.; Soto-Otero, R.; Méndez-Álvarez, E.; Thull, U.; Testa, B.; Altomare, C. Synthesis and Monoamine Oxidase Inhibitory Activity of New Pyridazine-, Pyrimidine- and 1,2,4-Triazine-Containing Tricyclic Derivatives. *J. Med. Chem.* **2007**, *50*, 5364–5371.
- (33) Rivara, S.; Piersanti, G.; Bartoccini, F.; Diamantini, G.; Pala, D.; Riccioni, T.; Stasi, M. A.; Cabri, W.; Borsini, F.; Mor, M.; Tarzia, G.; Minetti, P. Synthesis of (E)-8-(3-Chlorostyryl)caffeine Analogues Leading to 9-Deazaxanthine Derivatives as Dual A2A Antagonists/MAO-B Inhibitors. *J. Med. Chem.* **2013**, *56*, 1247–1261.
- (34) George, T.; Kaul, C. L.; Grewal, R. S.; Tahilramani, R. Antihypertensive and monoamine oxidase inhibitory activity of some derivatives of 3-formyl-4-oxo-4*H*-pyrido[1,2-*a*]pyrimidine. *J. Med. Chem.* **1971**, *14*, 913–915.
- (35) Yang, M.; Culhane, J. C.; Szewczuk, L. M.; Gocke, C. B.; Brautigam, C. A.; Tomchick, D. R.; Machius, M.; Cole, P. A.; Yu, H. Structural basis of histone demethylation by LSD1 revealed by suicide inactivation. *Nat. Struct. Mol. Biol.* **2007**, *14*, 535–539.
- (36) Binda, C.; Valente, S.; Romanenghi, M.; Pilotto, S.; Cirilli, R.; Karytinos, A.; Ciossani, G.; Botrugno, O. A.; Forneris, F.; Tardugno, M.; Edmondson, D. E.; Minucci, S.; Mattevi, A.; Mai, A. Biochemical, Structural, and Biological Evaluation of Tranylcypromine Derivatives as Inhibitors of Histone Demethylases LSD1 and LSD2. *J. Am. Chem. Soc.* **2010**, *132*, 6827–6833.
- (37) Ueda, R.; Suzuki, T.; Mino, K.; Tsumoto, H.; Nakagawa, H.; Hasegawa, M.; Sasaki, R.; Mizukami, T.; Miyata, N. Identification of Cell-Active Lysine Specific Demethylase 1-Selective Inhibitors. *J. Am. Chem. Soc.* **2009**, *131*, 17536–17537.
- (38) Binda, C.; Valente, S.; Romanenghi, M.; Pilotto, S.; Cirilli, R.; Karytinos, A.; Ciossani, G.; Botrugno, O. A.; Forneris, F.; Tardugno, M.; Edmondson, D. E.; Minucci, S.; Mattevi, A.; Mai, A. Biochemical, Structural, and Biological Evaluation of Tranylcypromine Derivatives as Inhibitors of Histone Demethylases LSD1 and LSD2. *J. Am. Chem. Soc.* **2010**, *132*, 6827–6833.

- (39) Mimasu, S.; Umezawa, N.; Sato, S.; Higuchi, T.; Umehara, T.; Yokoyama, S. Structurally Designed *trans*-2-Phenylcyclopropylamine Derivatives Potently Inhibit Histone Demethylase LSD1/KDM1. *Biochemistry* **2010**, *49*, 6494–6503.
- (40) Liang, Y.; Quenelle, D.; Vogel, J. L.; Mascaro, C.; Ortega, A.; Kristie, T. M. A Novel Selective LSD1/KDM1A Inhibitor Epigenetically Blocks Herpes Simplex Virus Lytic Replication and Reactivation from Latency. *mBio* **2013**, *4*, e00558–e005512.
- (41) Rotili, D.; Tomassi, S.; Conte, M.; Benedetti, R.; Tortorici, M.; Ciossani, G.; Valente, S.; Marrocco, B.; Labella, D.; Novellino, E.; Mattevi, A.; Altucci, L.; Tumber, A.; Yapp, C.; King, O. N. F.; Hopkinson, R. J.; Kawamura, A.; Schofield, C. J.; Mai, A. Molecular Hybridization: A Useful Tool in the Design of New Drug Prototypes., Pan-Histone Demethylase Inhibitors Simultaneously Targeting Jumonji C and Lysine-Specific Demethylases Display High Anticancer Activities. *J. Med. Chem.* **2014**, *57*, 42–55.
- (42) Sharma, S. K.; Wu, Y.; Steinbergs, N.; Crowley, M. L.; Hanson, A. S.; Casero, R. A.; Woster, P. M. (Bis)urea and (Bis)thiourea Inhibitors of Lysine-Specific Demethylase 1 as Epigenetic Modulators. *J. Med. Chem.* **2010**, *53*, 5197–5212.
- (43) Huang, Y.; Greene, E.; Murray Stewart, T.; Goodwin, A. C.; Baylin, S. B.; Woster, P. M.; Casero, R. A. Inhibition of lysine-specific demethylase 1 by polyamine analogues results in reexpression of aberrantly silenced genes. *Proc. Natl. Acad. Sci. U. S. A.* **2007**, *104*, 8023–8028.
- (44) Huang, Y.; Stewart, T. M.; Wu, Y.; Baylin, S. B.; Marton, L. J.; Perkins, B.; Jones, R. J.; Woster, P. M.; Casero, R. A. Novel Oligoamine Analogues Inhibit Lysine-Specific Demethylase 1 and Induce Reexpression of Epigenetically Silenced Genes. *Clin. Cancer Res.* **2009**, *15*, 7217–7228.
- (45) Culhane, J. C.; Szewczuk, L. M.; Liu, X.; Da, G.; Marmorstein, R.; Cole, P. A. A Mechanism-Based Inactivator for Histone Demethylase LSD1. *J. Am. Chem. Soc.* **2006**, *128*, 4536–4537.
- (46) Szewczuk, L. M.; Culhane, J. C.; Yang, M.; Majumdar, A.; Yu, H.; Cole, P. A. Mechanistic Analysis of a Suicide Inactivator of Histone Demethylase LSD1. *Biochemistry* **2007**, *46*, 6892–6902.
- (47) Culhane, J. C.; Wang, D.; Yen, P. M.; Cole, P. A. Comparative Analysis of Small Molecules and Histone Substrate Analogues as LSD1 Lysine Demethylase Inhibitors. *J. Am. Chem. Soc.* **2010**, *132*, 3164–3176.
- (48) Claudio, V.-J.; Amanda, D.; Vanderlan da Silva, B.; Eliezer, J. B.; Carlos Alberto Manssour, F. Molecular Hybridization: A Useful Tool in the Design of New Drug Prototypes. *Curr. Med. Chem.* **2007**, *14*, 1829–1852.
- (49) Jones, L. H.; Allan, G.; Barba, O.; Burt, C.; Corbau, R.; Dupont, T.; Knöchel, T.; Irving, S.; Middleton, D. S.; Mowbray, C. E.; Perros, M.; Ringrose, H.; Swain, N. A.; Webster, R.; Westby, M.; Phillips, C. Novel Indazole Non-Nucleoside Reverse Transcriptase Inhibitors Using Molecular Hybridization Based on Crystallographic Overlays. *J. Med. Chem.* **2009**, *52*, 1219–1223.
- (50) dos Santos, J. L.; Lanaro, C.; Lima, L. d. M.; Gambero, S.; Franco-Penteado, C. F.; Alexandre-Moreira, M. S.; Wade, M.; Yerigenahally, S.; Kutlar, A.; Meiler, S. E.; Costa, F. F.; Chung, M. Design, Synthesis, and Pharmacological Evaluation of Novel Hybrid Compounds To Treat Sickle Cell Disease Symptoms. *J. Med. Chem.* **2011**, *54*, 5811–5819.
- (51) Valli, M.; Danuello, A.; Pivatto, M.; Saldana, J. C.; Heinzen, H.; Domínguez, L.; Campos, V. P.; Marqui, S. R.; Young, M. C. M.; Viegas, C., Jr; Silva, D. H. S.; Bolzani, V. S. Anticholinesterasic, Nematostatic and Anthelmintic Activities of Pyridinic and Pyrazinic Compounds. *Curr. Med. Chem.* **2011**, *18*, 3423–3430.
- (52) Patpi, S. R.; Pulipati, L.; Yogeeshwari, P.; Sriram, D.; Jain, N.; Sridhar, B.; Murthy, R.; T, A. D.; Kalivendi, S. V.; Kantevari, S. Design, Synthesis, and Structure–Activity Correlations of Novel Dibenzo-[*b,d*]furan, Dibenzo[*b,d*]thiophene, and N-Methylcarbazole Clubbed 1,2,3-Triazoles as Potent Inhibitors of *Mycobacterium tuberculosis*. *J. Med. Chem.* **2012**, *55*, 3911–3922.
- (53) Sashidhara, K. V.; Kumar, M.; Khedgikar, V.; Kushwaha, P.; Modukuri, R. K.; Kumar, A.; Gautam, J.; Singh, D.; Sridhar, B.; Trivedi, R. Discovery of Coumarin–Dihydropyridine Hybrids as Bone Anabolic Agents. *J. Med. Chem.* **2013**, *56*, 109–122.
- (54) Ma, L.-Y.; Pang, L.-P.; Wang, B.; Zhang, M.; Hu, B.; Xue, D.-Q.; Shao, K.-P.; Zhang, B.-L.; Liu, Y.; Zhang, E.; Liu, H.-M. Design and synthesis of novel 1,2,3-triazole-pyrimidine hybrids as potential anticancer agents. *Eur. J. Med. Chem.* **2014**, *86*, 368–380.
- (55) Skulnick, H. I.; Ludens, J. H.; Wendling, M. G.; Glenn, E. M.; Rohloff, N. A.; Smith, R. J.; Wierenga, W. Pyrimidinones. 3. N-Substituted 6-phenylpyrimidinones and pyrimidinediones with diuretic/hypotensive and antiinflammatory activity. *J. Med. Chem.* **1986**, *29*, 1499–1504.
- (56) Hu, M.; Li, J.; Q. Yao, S. In Situ “Click” Assembly of Small Molecule Matrix Metalloprotease Inhibitors Containing Zinc-Chelating Groups. *Org. Lett.* **2008**, *10*, 5529–5531.
- (57) Wilkening, I.; Signore, G. d.; Hackenberger, C. P. R. Synthesis of phosphonamidate peptides by Staudinger reactions of silylated phosphinic acids and esters. *Chem. Commun.* **2011**, *47*, 349–351.
- (58) Zheng, Y.-C.; Duan, Y.-C.; Ma, J.-L.; Xu, R.-M.; Zi, X.; Lv, W.-L.; Wang, M.-M.; Ye, X.-W.; Zhu, S.; Mobley, D.; Zhu, Y.-Y.; Wang, J.-W.; Li, J.-F.; Wang, Z.-R.; Zhao, W.; Liu, H.-M. Triazole–Dithiocarbamate Based Selective Lysine Specific Demethylase 1 (LSD1) Inactivators Inhibit Gastric Cancer Cell Growth, Invasion, and Migration. *J. Med. Chem.* **2013**, *56*, 8543–8560.
- (59) Ferrari-Amorotti, G.; Fragliasso, V.; Esteki, R.; Prudente, Z.; Soliera, A. R.; Cattelani, S.; Manzotti, G.; Grisendi, G.; Dominici, M.; Pieraccioli, M.; Raschellà, G.; Chiodoni, C.; Colombo, M. P.; Calabretta, B. Inhibiting Interactions of Lysine Demethylase LSD1 with Snail/Slug Blocks Cancer Cell Invasion. *Cancer Res.* **2013**, *73*, 235–245.